A Hydrodynamic Interpretation of the Tapeats Sandstone

Part I: Basal Tapeats

W.R. Barnhart*

Abstract

The Tapeats Sandstone is the lowest Cambrian layer in the Grand Canyon in Arizona. It has been interpreted as beach, estuarine, and shallow marine coarse sand deposits, representing the initial stages of a slow transgression over a highly weathered and eroded, pre-vegetated epicratonic surface. In the basal Tapeats, two distinct bedforms occur: (1) hyperconcentrated laminar bedforms deposited by high-velocity hyperconcentrated currents and (2) sandy debris flows in high-density turbulent flow. The high-velocity hyperconcentrated currents predominated, but were occasionally interrupted or overlaid by cascades of breccia that initiated short-lived, high-density turbulent flow. Both reflect extremely rapid deposition rather than tidal reworking on a passive margin. Rheologically plastic flows are distinct from fluidal flows. The structure of high-density turbidity currents and hyperconcentrated flood flows are discussed, showing how the hyperconcentrated laminar bedforms and sandy debris flows could have been produced. Hydrological interpretation indicates that bedforms were produced by very rapid deposition in continuous currents over an extremely large area without regard for minor paleotopography, suggesting the rapid transgression of the Tapeats Sandstone in a massive flooding event.

Introduction

The Tapeats Sandstone is the lowest formation of the Paleozoic Tonto Group at Grand Canyon. Named for exposures along Tapeats Creek by Noble in 1914, this sandstone formation and the overlying Bright Angel Shale and Mauve Limestone (Figure 1) have been classified as Cambrian since the classic work of Walcott (1890).

Cambrian deposits in the Grand Canyon and throughout the Rocky Mountains long have been cited as representing a classic transgressive sequence of sandstone, mudstone, and limestone that accumulated on the slowly subsiding Cordilleran miogeocline and adjacent craton. Shoreline migration for the most part was eastward, resulting in deposition

* W.R. Barnhart, c/o Creation Research Society, Chino Valley, AZ
Accepted for publication May 17, 2011

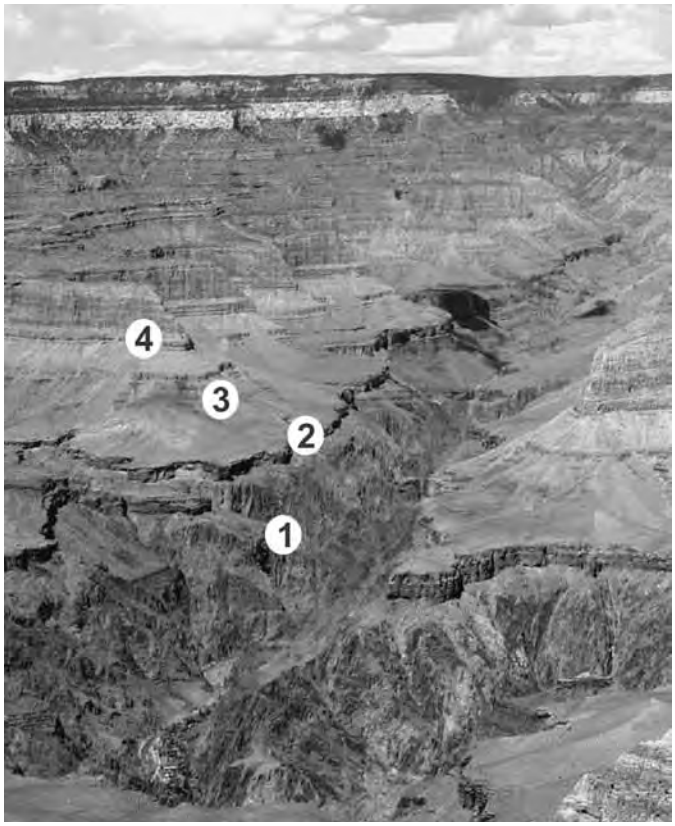

Figure 1. Overview of Grand Canyon showing Cambrian strata in context. 1 = Vishnu Schist; 2 = Tapeats Sandstone; 3 = Bright Angel Shale; 4 = Mauve Limestone. From http://thevibe.socialvibe.com/wp-content/uploads/2009/01/arizona-grand-canyon-vista.jpg (accessed December 2010)

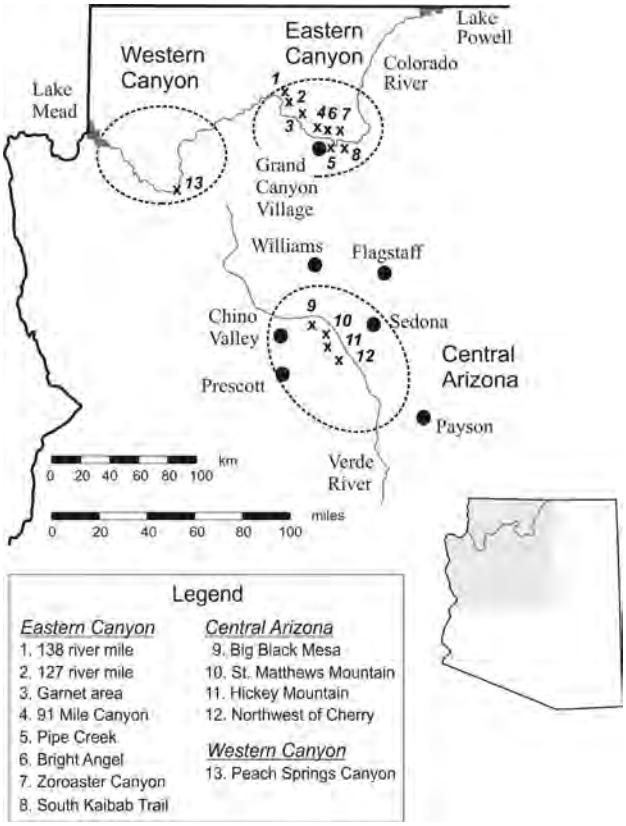

Figure 2. Areas of exposure of Tapeats Sandstone in Arizona, USA. Three major locations include: western canyon, eastern canyon, and central Arizona. Major monadnock locations are labeled showing the north-south alignment.

> of coarse clastics in shallow water areas to the east and finer clastics and carbonates in more offshore areas to the west (Middleton and Elliott, 2003, p. 90).

In the eastern Grand Canyon and central Arizona region (Figure 2) the Tapeats is interrupted by numerous monadnocks—irregular hills or highs in the Precambrian surface, some extending into the Bright Angel Shale. These are often associated with deposits of loose breccia, apparently eroded from the monadnocks, which cover the bases and sides of the hills, reaching 50 ft (15.3 m) in thickness (Middleton and Elliott, 2003). These monadnocks were interpreted as paleohills by McKee (1945) and many others, who imagined the Tapeats depositional environment as a broad beach gradually covering the ancient topography, migrating over rising land to the northeast (Hereford, 1977; Rose, 2006).

Within that general uniformitarian concept, various ideas have been advanced for deposition in estuaries, on beaches, and in shallow marine offshore environments, resulting in a variety of facies models for the Tapeats. McKee (1945) viewed it as a subtidal deposit with sediment arriving from the northeast to be reworked by tidal action in water less than 50–60 ft (15.3–18.3 m) deep. Wanless (1973), based on the occurrence of "fenestrated fabrics and dessication cracks" (Middleton and Elliott, 2003, p. 95) in the Mauve Limestone, suggested at least part of the Tonto Group was deposited subaerially. Hereford (1977, p. 201, 203, 209, brackets added), working Tapeats outcrops in central Arizona (Figure 2), used "more than 800 orientation measurements" to conclude that "the average direction of sediment transport was west-southwest" and "deposited primarily on sandy intertidal flats … governed by the diminishing energy of tidal currents flowing shoreward across the gently-sloping tidal flats" with a tidal range of "between 5 and 10 m [16.4 and 32.8 feet]."

Others have suggested that some Tapeats facies have nothing to do with nearshore environments. Chadwick and Kennedy (2001, pp. 3, 4, brackets added) recognized that the "breccia extend for

vertical distances of up to 140 meters [460 ft]" and "exhibit no evidence of post-depositional erosion or reworking prior to burial." They posited that "the widespread preservation of the breccia would require that … the unit existed below wave base," with a "water depth up to 200 meters [656 ft]." Berthault (2004, p. 481) thought that the Tonto Group originated initially "with the powerful current that eroded the granites and schist" of the Precambrian basement. As this erosive current, proceeding from west to east "advanced, the water depth increased, resulting in reduction of the current. The ensuing regressive current carried westward the largest particles in a bedload and the smaller ones in a suspended load." He suggested that Tonto Group deposition derived from this decreasing velocity current in one depositional episode.

While various authors have looked to facies to interpret the Tapeats, this study will instead examine hydrodynamics as a basis for interpretation, following the work of Barnhart (2011b), who showed that facies models could not explain the splay deposits of Hurricane Katrina. Sediments that would typically be attributed to repeated crevasse or overbank sedimentation in a deltaic environment were actually the result of a single depositional episode caused by catastrophic breaching of a levee in New Orleans. This mistake can be traced to the quasi-uniformitarian expectation that sediments are laid down under normal equilibrium conditions for particular facies. However, hydrodynamic studies of the individual layers demonstrated that strata were laid under catastrophic conditions, with little connection to the suggested facies, indicating that facies models can act as barriers to understanding the rock record.

Using a hydrodynamic approach, this series will take a new look at the Tapeats Formation. It will argue that layers within the Tapeats were deposited in hyperconcentrated flow conditions under an upper flow regime, with bedform height governed by flow depth. Determination of sediment concentration and rheological conditions will shed light on sedimentation rate, current velocity, and water depth during deposition. This is an introductory study and will not describe and interpret each layer of the Tapeats, but will instead provide an overview based on selected outcrops examined by the author. All bedforms suggest rapid deposition under extreme conditions: an overlay of storm waves on a violent flooding event resulted in continuous flooding onto a rapidly accreting surface, with limited evidence of reworking by the sediment-rich current, and no evidence of reworking by tidal currents.

This first paper will deal with the basal Tapeats—those layers immediately overlying the Great Unconformity. I will attempt to demonstrate that these layers were deposited under plastic flow conditions, affected by associated monadnocks and breccia flows caused by cascades of previously eroded rubble off of topographic highs. The second paper will deal with the middle and upper Tapeats; those layers are commonly cross-bedded and were probably deposited in a rheological regime of fluidal flow. Despite many incised channels and evidence of bidirectional flow, they were not deposited by tidal currents but by continued catastrophic flooding.

Hyperconcentrated Flood Flows and Debris Flows

The basal Tapeats in much of the eastern Grand Canyon is described by Chadwick and Kennedy (2001, p. 3, brackets added) as "alternating of light and dark layers of well-sorted graded sandstone beds. The debris flows [of breccia] generally lie immediately above these Tapeats beds." They cite Burgert (1972), who described these layers as turbidites. His attribution is unique and not cited in any other paper seen by the author. Hereford (1977, pp. 204, 206, brackets added) saw these strata that were "mapped by McKee … in the eastern Grand Canyon National Park" as his facies C, described as

> low (2°–10°) to medium (10°–20°) cross stratification, trough cross-stratification, tangential foresets, no alternation of coarse-fine foresets, continuous parallel stratification. Medium to coarse sandstone [0.24–0.48 mm], well sorted, pale red.

While I will differ with Hereford's (1977) facies approach, his "facies C" is comparable to the basal Tapeats layers analyzed below. But as McKee et al (1967, p. 850) observed after their work on the flood deposits of Bijou Creek, Colorado, "much of the layering is in the form of fine laminae similar to the type commonly ascribed to intermittent accumulation in quiet water over a long period of time."

This is a wise precaution as we consider a formation that most authors assume was deposited grain by grain under normal fluidal flow.

Were the basal Tapeats bedforms (Figure 3 and 4) produced by normal fluidal flow, where a grain-by-grain pattern of sedimentation occurs? In that situation, flow is fully turbulent and individual grains are deposited from bedload or suspension as they independently interact with turbulence vectors (Smith, 1986). Another possibility was noted by Smith (1986), who described sediment movement in hyperconcentrated flood flows. These are not fully turbulent, but sediment is partly supported by dispersive pressure (interaction between grains) and buoyancy. For example, the addition of as little as 2% colloidal clay or very fine sand can raise the fluid viscosity. He described hyperconcentrated flood flows as having 40–80% solids by volume (about 22–62% by weight) (Julien, 1998), suggesting significant sediment concentrations.

Smith (1986) thought that hyperconcentrated flood flow was intermediate

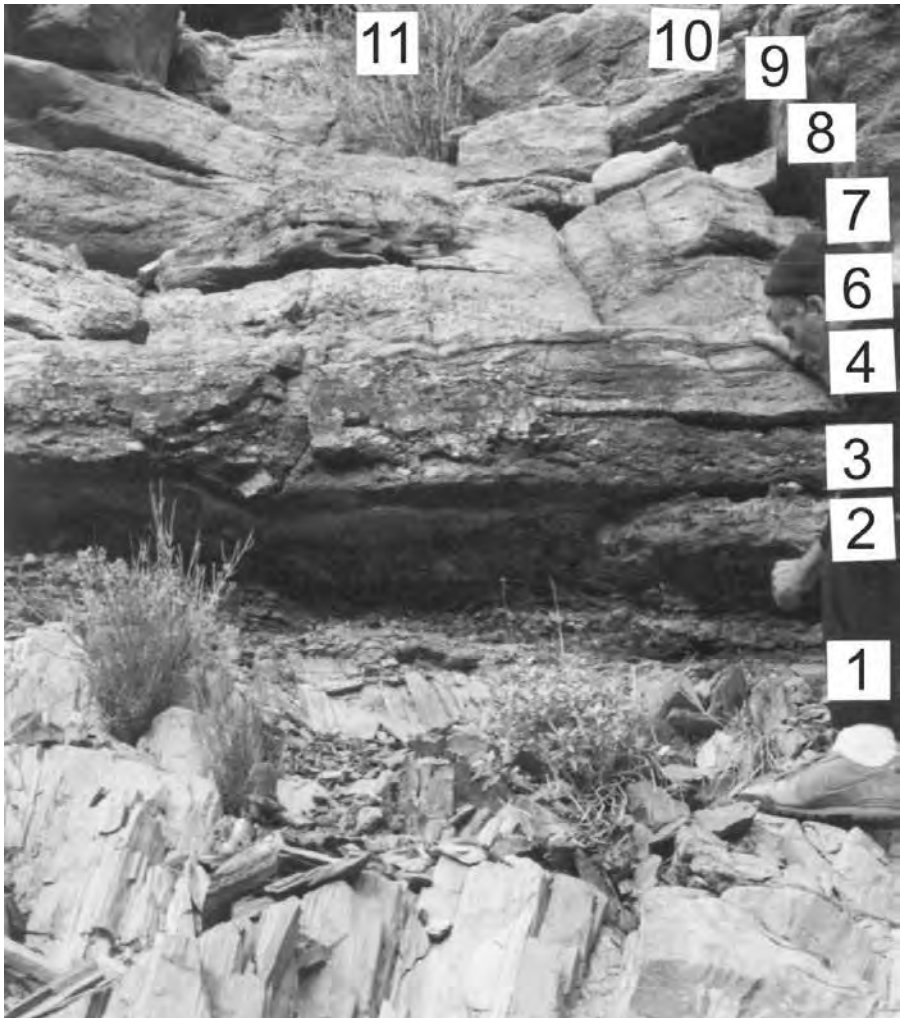

Figure 3. Great Unconformity and basal Tapeats Sandstone, Boucher Cabin site, Boucher Trail. Breccia at the contact is mica schist, similar to the substrate, the Vishnu Schist. Numbers show individual bedforms: (1) Clast supported with sand matrix. Material flowed downward to fill cracks and upwards to face layers 3 and 4 while still plastic. (2) Matrix supported conglomerate that terminates mid photo. (3) Higher proportion sand matrix with scattered clasts. (4) Sand layer with few small clasts. Intrusion of (1) covers face as a result of loading. (5) Layer is lens to right obscured by person. (6–7) Sand matrix with visible, 3–5 mm, ferruginous purple inclusions. (8) Cross bedded sand. (9–11) Laminar sand layers. See text for details.

between normal fluidal flow and fully plastic flow. Greater concentrations of sediment would cause deposition *en masse*. Shanmugam (1996) attributed a more plastic flow as the cause of what he called "sandy debris flows." Sandy debris flows can be identified by rafted large clasts transported by the flow density, inverse grading of entrained clasts toward the center of the flow, thoroughly mixed clasts and matrix, and the abrupt freezing of flows during deposition (Figures 5 and 6).

In the cross section of the basal Tapeats seen in Figure 3 from Boucher's cabin site (Figure 7), a variety of depositional products are observed, but none were caused by fluidal flow. A monadnock influences sedimentation here; although not immediately visible, its effects are evidenced in the first few layers, and the paleohill is either within the rock face or once existed in the open space behind the viewer.

The layer of breccia (Figure 3, Layer 1) was a product of localized erosion, as seen by the similarity of its small angular clasts of mica schist to the local substrate. This type of rubble field generally indicates an adjacent monadnock—the source of the eroded breccia. McKee (1945) recognized this association and assumed it originated from wave action against a monadnock, like that seen today where waves pound into marginal highlands. But that environment, implying lengthy time, would have rounded the clasts, which are soft. However, field observation shows sharp, crisply broken surfaces, indicating a very short period between erosion and burial of these breccia clasts.

At this location, it appears obvious that the basal Tapeats is not a beach deposit. There is no evidence of repeated wave action reworking sediment. Layer 2 was deposited, not grain by grain as fluidal flow, but as a presorted set of sediments in a high-density flow. It was initially deposited over the breccia of Layer 1 as plastic flow, and the absence of mixed breccia up into the sand shows no reworking. Even a single tidal cycle, with numerous waves pounding the gravel beach would have produced mixing. The small amount of breccia entrained in Layer 2 can be better explained as a small turbulence created by the arrival of a single wave whose actions were limited by the definite separation between Layers 1 and 2. Entrained breccia clasts are limited to the lowermost part of Layer 2; note their absence above the individual's left fist, barely 1 meter away from Layer 1 on the left. This indicates that the current's turbulent energy was dedicated to carrying sediment (Schumm and Kahn,

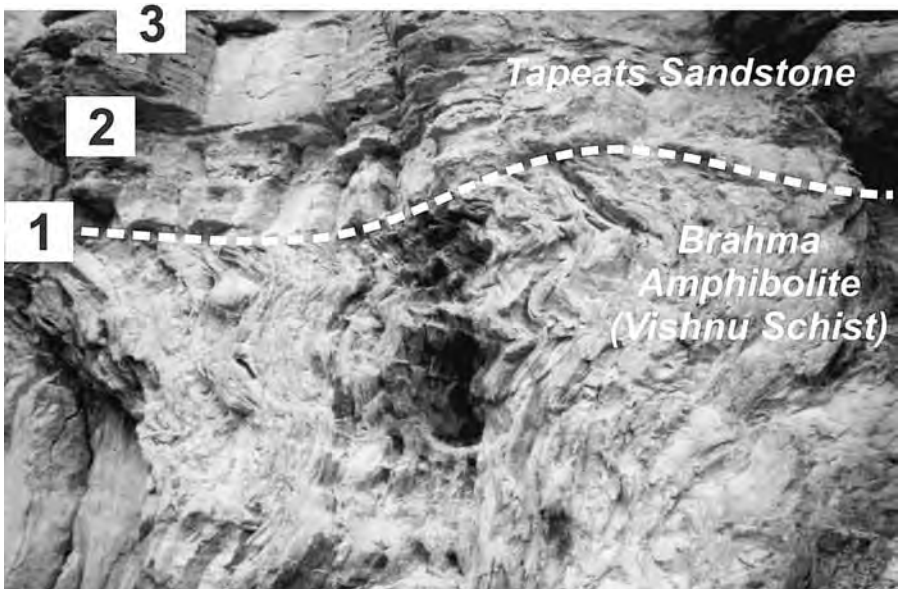

Figure 4. Great Unconformity and basal Tapeats Sandstone, Clear Creek Trail, about 1 km east of Phantom Ranch and Bright Angel Creek. (1) Great Unconformity. (2–3) Divisions between hyperconcentrated laminar layers of Tapeats. Scale = ~1.5 m across field of view.

1972). Its concentration of solids was sufficiently high to preclude any erosion by its turbulent head (Figure 8.3). There were no lapping waves; the continuing high current velocity was depositing high flow regime flat beds in the form of hyperconcentrated laminar flat beds.

Layer 3 contains a rectangular clast, 3 x 5 cm, the less dense mica schist. This clast was embedded in the lowest part of the layer as it rose and thinned over the monadnock. The entrained clasts are only about 1 cm (intermediate diameter, or d_B). These clasts moved only a short distance, once again illustrating the lack of repeated mixing and, therefore, turbulent flow in the current.

Layers 2 and 3 show unique elliptical internal fractures not seen in overlying layers. It is not clear if this is the convex dish structures cited in some accounts

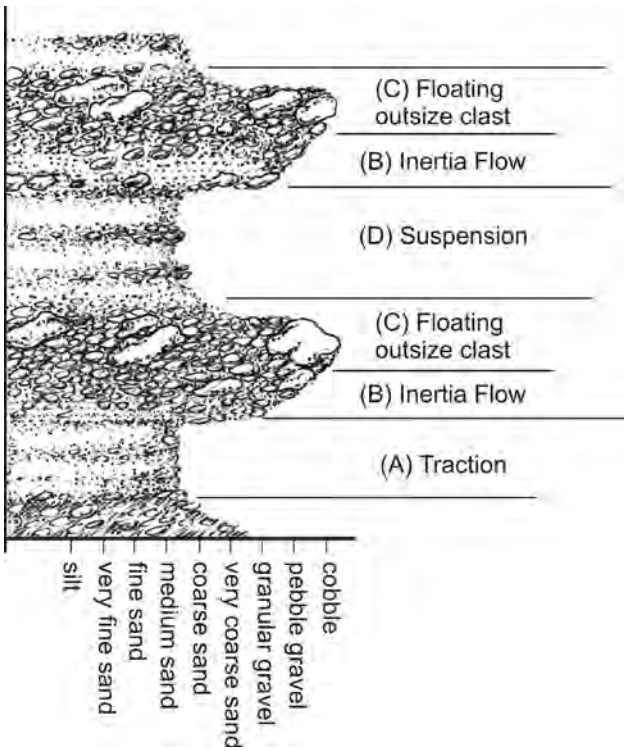

Figure 5.1. Idealized debris flow cross section as seen in combination of two examples interpreted as fan deltas. Labeling is a reflection of the part of the flow that deposited the section. C-B = reverse grading; D-C = normal grading. After figure 4 in Shanmugam (1996).

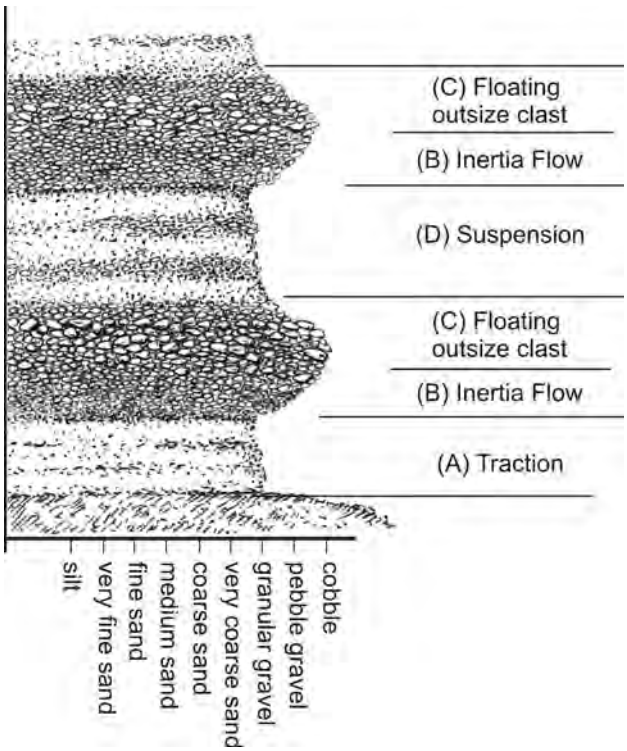

Figure 5.2. Sandy debris flow deposits in cross section. All clast sizes reduced to reflect the small differences in size between coarse sand and small pebbles. After figure 4 in Shanmugam (1996).

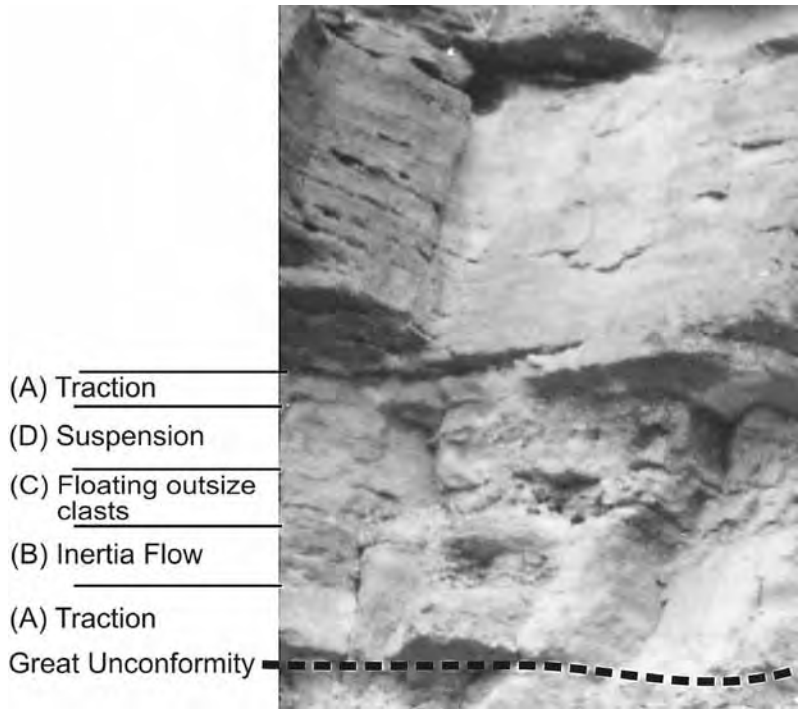

Figure 6. Upper left corner of Figure 4. A debris flow showing the same sublayers as Figure 5.

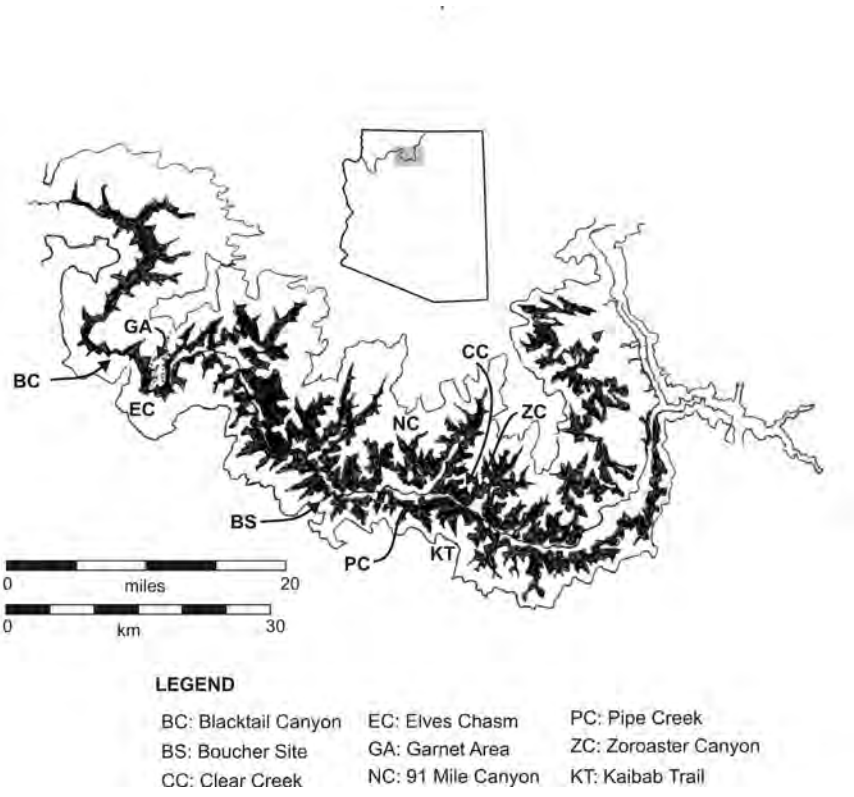

Figure 7. Locations in eastern Grand Canyon discussed in this paper. Dark areas represent exposures of Tapeats Sandstone and Bright Angel Shale. After figure 1 in Rose (2006).

of debris flows (Shanmugam, 1996), or incipient convoluted bedding per McKee et al. (1967), or an indication of decreased velocity of the hyperconcentrated flow (Barnhart, 2011b). To the left of the figure in layer 3, a distinct grouping of larger clasts can be seen in the middle of the layer. Floating clasts in the center of a layer is one of the distinct characteristics of a debris flow (Figure 5.2), where they ride on the increased density of the Inertia Flow (laminar flow) layer and under the bottom of the suspension (turbulent flow) layer. A visible inverse grading can be seen below the center, representing the laminar flow and normal grading from the turbulent, or suspension, flow overlays it up to the prominent light layer of white sand that would be in the right position for the traction band overlying Layer 4. A similar thin light layer can be seen under the ledge of Layer 3 and at the top of Layer 4. These distinct layers of white sand are interspersed between layers of sandy debris flows throughout the basal Tapeats. They appear to be a product of suction in the head of the high-density turbulent flow that has suspended the sediment in the viscous sublayer, sufficient to separate the finer fraction of white sand, and then relay it down flow as the sediment of the debris flow deflected the turbulence (Figure 8.3). The occurrence of a distinct, continuous traction layer indicates recurring adequate separation between depositional pulses in the flow to provide a break in sedimentation.

Shanmugam's (1996) diagram (Figure 5.1) illustrates these bands in the debris flows containing clasts of a broad size range. In the basal Tapeats, however, sediment distribution was limited by the sediments that were entrained. If a full range of clast sizes are not available, debris flow deposits will lack the clarity, as seen in Figure 5.2.

While Layers 2 and 3 show faint but well organized internal layering, Layer 4 and those above it show considerably more, though less regularly organized.

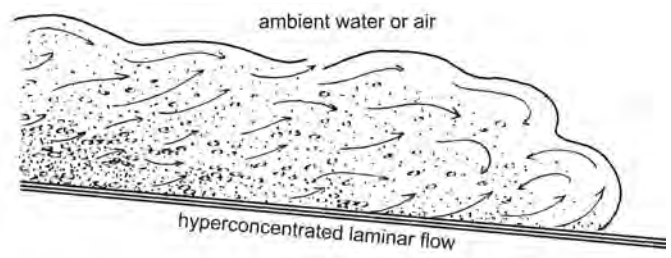

Figure 8.1. Hyperconcentrated flood flow as it would deposit hyperconcentrated laminar bedforms. Differs from high-density turbulent flow because all turbulence originates from substrate contact without significant turbulence generated at contact with ambient air or water. Note that no direction is inferred for Tapeats deposition in Figures 8.1–8.4.

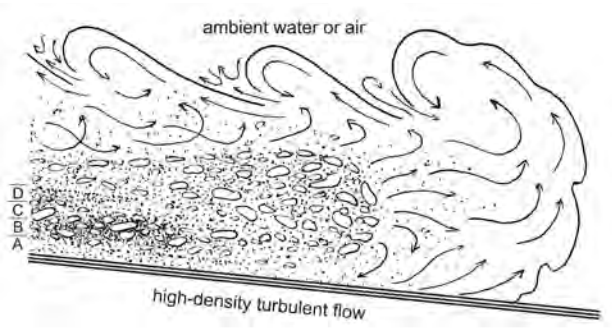

Figure 8.2. High-density turbulent flow in cross section as it would deposit a sandy debris flow based on high-density turbidites of larger clast size. Letters to left designate layers corresponding to those in Figure 5.1 After figure 4 in Shanmugam (1996).

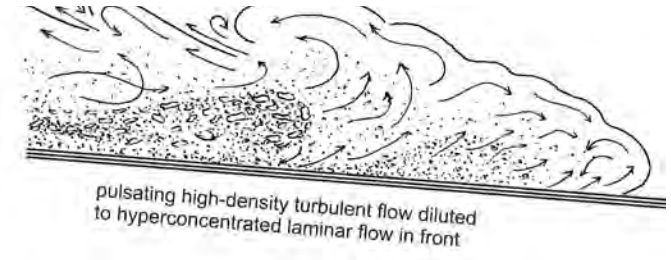

Figure 8.3. Effects of pulsation in high-density turbulent flow would produce stacked bedforms. Formation of traction layer A requires pulse separation to allow settling of fines or pulses of sediment hydroplaning over the compressed layer of the inertia flow. After Sohn et al. (2002, their figure 1). Drawing horizontally compressed to show multiple pulses.

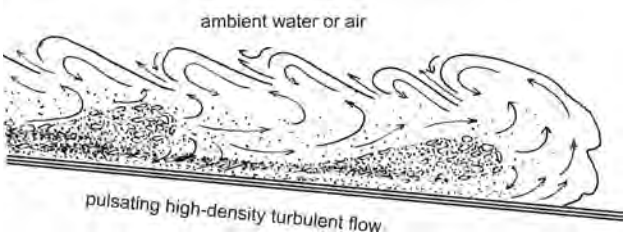

Figure 8.4. Pulses in high-density turbulent flow do not necessarily dilute to hyperconcentrated laminar flow at the leading edge, as in Figure 8.3. After figure 1 in Sohn et al. (2002). Drawing horizontally compressed to show multiple pulses.

These bedforms are similar to splay deposits formed during levee breaches in New Orleans during Hurricane Katrina (Barnhart, 2011b, his figure 7) and interpreted as hyperconcentrated laminar bedforms. Similar irregular, layered bedding is seen in the Toutle River valley west of Mount St. Helens (Figure 9), having formed by flooding following the May 1980 eruption (Smith, 1986) and sediments deposited at Bijou Creek, Colorado during the floods of June 1963 (McKee et al, 1967, their figures 5 and 7). Discontinuous laminae—<1 cm up to 3 cm thick—comprise each layer. The basal Tapeats contains a mixture of white sand laminae, medium-to-coarse white sand bedding, and a dark red to purple sand (sometimes called magenta or red sand) (Noble, 1922). McKee (1945) identified the dark sand as ferruginous sand, and Elston and Bessler (1977) identified the iron as syndepositional with the sand, not a diagenetic product. All of it occurs (Figure 10) at lower Elves Chasm Falls (Figure 7), just a few meters above the Great Unconformity. The lack of obvious patterns in the predominantly purple sediments demonstrates that sedimentary units are a product of the sediment entrained in the transporting current. Figure 11.1 shows the ubiquitous mixing of white and purple sediments at both the bottom and top of the section captured in that figure.

Hyperconcentrated flow deposits have been studied in subariel volcanic debris fields. Though there is no known volcanism associated with the Tapeats, the hydrodynamic principles behind the bedforms remain the same. They are typically more reliable than facies models in

Figure 9. Hyperconcentrated flood flow from Toutle River valley debris field of Mt. St. Helens. Later arrival of horizontal flood flow did not displace dark and light oblique layers of loose pyroclastic deposits from May 18, 1980 eruption. After figure 4B in Smith (1986). Note discontinuous nature of layering.

Figure 10. Close-up detail of laminar layers in lower Tapeats Sandstone. Mixing of purple ferruginous sand (gray bands) with white sand typical of such exposures. Modified from http://www.360parks.com/grand_canyon_colorado_river.shtml (accessed January 2011).

understanding the sedimentary process because hydrodynamic principles allow a quantitative assessment of actual depositional conditions, rather than some imagined "environment." Thus, the principles of hyperconcentrated flows in volcanic regimes can be applied to sedimentation in certain current conditions. Many hyperconcentrated flows begin as debris flows (Figure 8.2). Large debris flows can form with little water, but when they overflow into streams, lakes, snow packs, and other sources of water, they are diluted. The cogenetic contact of water and debris flow led Smith (1986) and Shanmugam (1996) to independently conclude that a debris flow would transform into a hyperconcentrated flood flow (Figure 8.1) when it entrained sufficient water to lubricate and dilute the flow. This situation would hold even for subaqueous debris flows (Figure 8.2), sometimes called hyperpycnal flow (a submerged high-density turbulent flow), where the turbulence is primarily restricted to its head and to the upper surface where ambient water is entrained.

Therefore, Layers 2 and 3 may represent debris flows where succeeding layers were deposited by the same current after it entrained sufficient water to dilute the slurry and change the rheological character of the flow.

In Figure 3, much of Layers 3 and 4 are hidden by a clastic veneer—a result of upward deformation of Layer 1. It is likely that overburden pressure was sufficient to crack brittle sandstone laminae, pressing them down into the still-plastic breccia. As a result, the plastic breccia migrated upward in response to loading. Such a sequence of events would have been rapid. Since the sandstone was already at least partially lithified when the overburden accumulated, then its initial cement would have been present as intergranular ions, possibly entrained in the flow itself. Cementation would have been quite rapid and not a result of slow percolation of later pore fluids. In that case, both the sandstone and the breccia would have been cemented, and the deformation observed would have been impossible.

Layer 6, with its many purple spots, strongly resembles Layer 1 of Figure 4. Both contain small voids, suggesting a similar origin for the layers. However, the deposits in Figure 4 and those in Figure 3 are about 16 km apart (Figure 7) and on opposite sides of the Colorado River. The small vugs often contain small secondary crystal growth, which suggests lithification before the deposit was compacted by overburden. If the vugs formed during deposition, then as a natural part of the lamination structure, the voids must have formed simultaneously with the bedform. That would preclude deposition grain by grain in a fluid flow, because the increased viscosity of the fluid due to fine sand in suspension would have prevented air from escaping (cf. Klein, 1970, his figure 15A).

We can only speculate about the original vug fill. It might have been original fluids, forming vugs during cementation, or just air bubbles, as documented by Klein (1970) in sediments deposited across the top of a sand bar in the Bay of Fundy, Nova Scotia, which I would interpret as hyperconcentrated laminar bedforms. Regardless of what they originally contained, they testify to the rapid deposition, burial, and lithification before loading of what was originally a cohesive plastic mass.

The upper layers (Layer 4 and above) were rapidly deposited by a hyperconcentrated flow (Smith, 1986). By analogy, it probably had a concentration of solids close to 20–30% by volume (Lowe, 1982; Barnhart, 2011b) or as high as 60% (Pierson and Costa, 1987).

Under these depositional conditions, it is likely that the laminar or bedding thickness is proportional to the depth of the depositing current. According to Allen (1976), this ratio would have been on the order of 6:1 to 8:1. Since Layer 4 is 12–16 cm thick, its depositing current would have been only 0.72–1.28 m deep. This is significantly less than the 50–60 feet of McKee (1945) or the 200 m of Chadwick and Kennedy (2001). The difference is based on the primacy of facies models and environmental conditions assumed by these authors, rather than a quantitative assessment

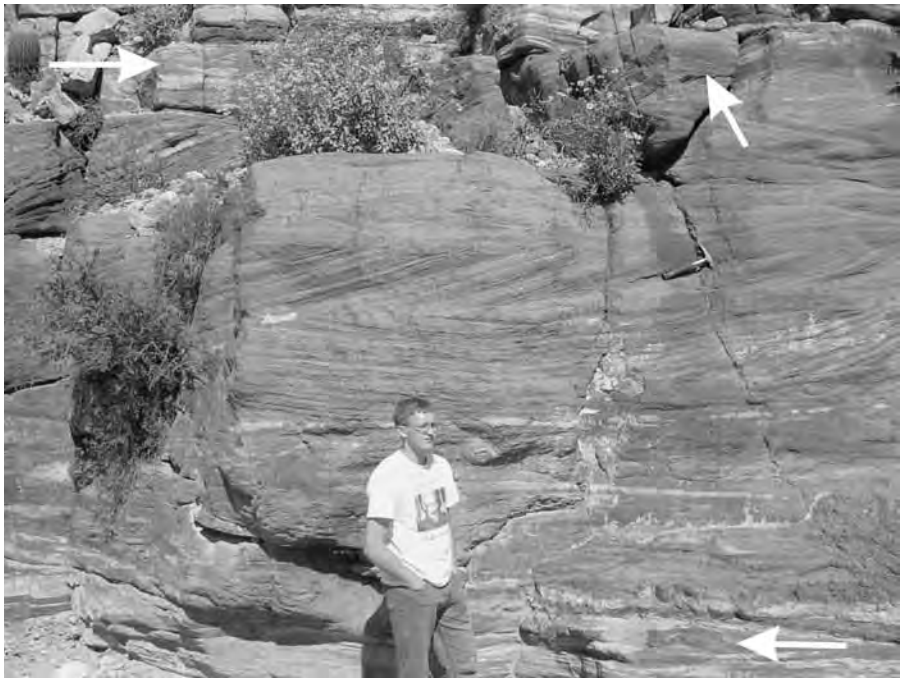

Figure 11.1. Tapeats Sandstone, labeled "Peach Spring Canyon" but with strata matching that east of Pipe Creek. Layers showing repeated hyperconcentrated laminar bedforms at the bottom and near top, with ferruginous (purple) sand (arrows) layered with white sand, traction layers. Cross bedding in center the result of sandy debris flows. From http://web.mst.edu/~rogersda/umrcourses/geo372/2005–03–27–109-Peach_Springs_Canyon-cross_bedding.JPG (accessed December 2010).

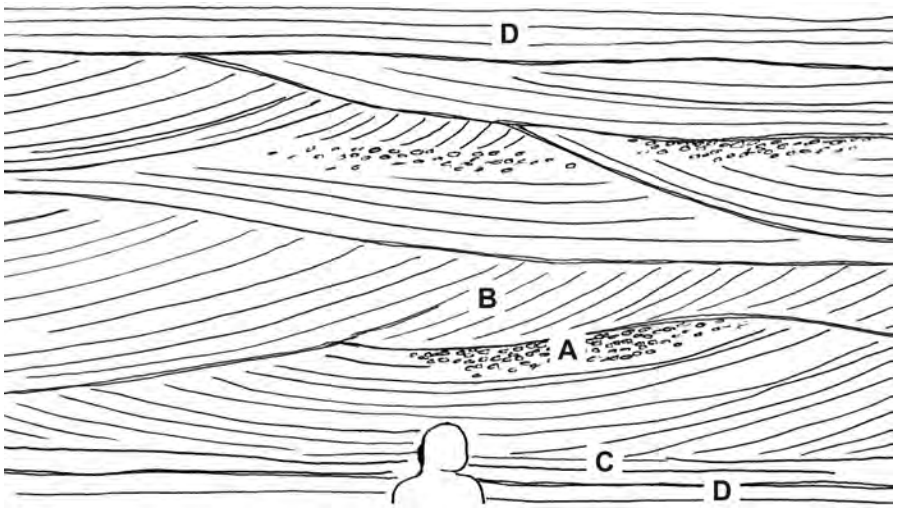

Figure 11.2. Sketch identifying: (A) disorganized outsized rafted clasts of coarse sand and small pebbles, (B) general trend of trough cross bedding, (C) traction layer of white sand at the bottom of trough cross bedding, or at the top of (D) hyperconcentrated laminar bedforms both below and above.

of hydrodynamics of the deposit itself. Those authors believed that the coarse sand was deposited below wave base in a marine environment. In contrast, this paper proposes that the layers reflect wave surges superimposed on a strong unidirectional current. Furthermore, high-velocity flat beds cannot form in deep water (McBride et al., 1975; Smith, 1971), which requires higher velocity to maintain competency (Grant, 1997). Rapidly accreting high-velocity flat beds typically do not form in deep water; instead, sediments are usually reworked at depth. Layers 6, 7, 9, and 10 are about the same thickness, suggesting shallower water persisted, probably over a broad area. This is similar to the Katrina splay deposits, which were influenced by the mass of Lake Pontchartrain, as well as by the width of the levee breaches. These factors influenced flow depth and rheology, and thus the resulting bedforms (Barnhart, 2011b). Layer 5 is not sufficiently visible to evaluate, and Layer 8 is appreciably thinner by contrast, showing another rhythmic pattern that will be discussed in the next paper of this series.

The visibility of the characteristics in the layers of Figure 3 result primarily from their location inside a large conchoidal overhang. Here, the rock fractured and broke loose along planes that reflect different stresses in each layer, suggesting distinct conditions for each layer.

These bedding differences are visible 24 km to the west at lower Elves Chasm (Figure 7). Figure 12 shows a part of an 8 m-tall exposure of the Tapeats on the right. Each layer was rounded by a current. These beds are stratigraphically higher, representing the transition up into the middle Tapeats, despite being only a few meters above the Great Unconformity. At this location, there is a greater variation in thickness of these beds, which are coated by desert varnish. Thickness varies from 1–16 cm, as seen at Boucher (Figure 3, Layer 8). That thickness variation is also visible in the

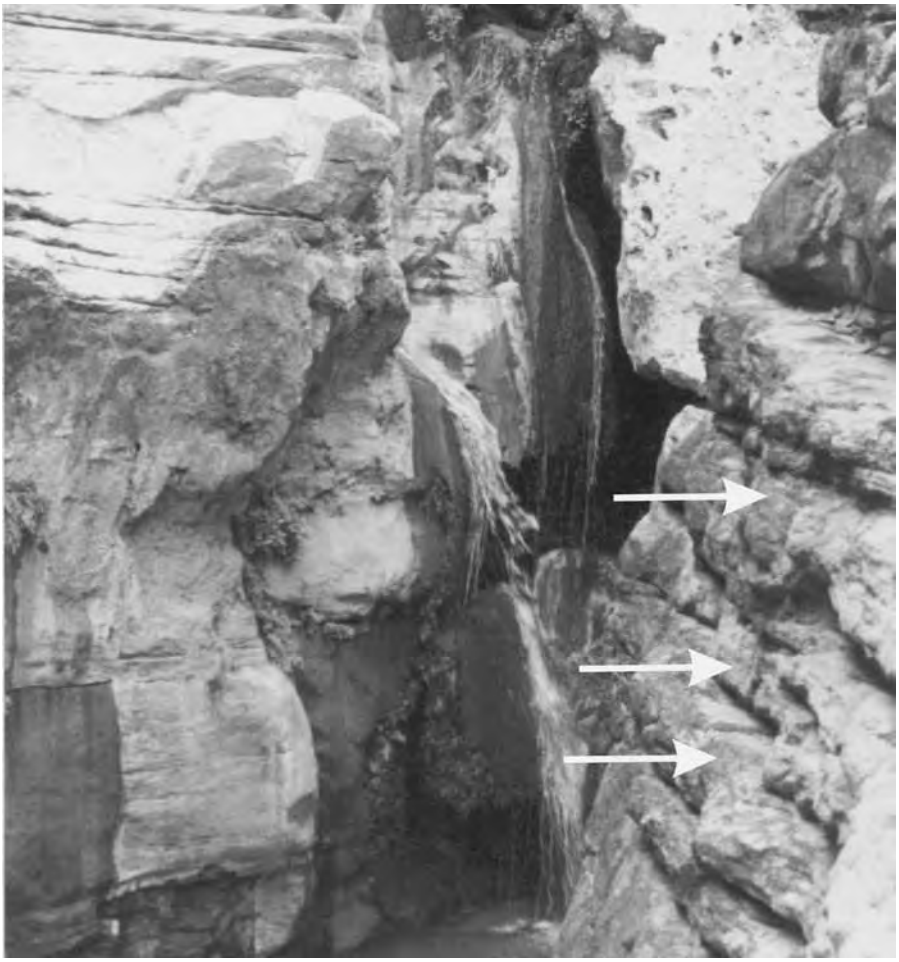

Figure 12. Laminar layers near the bottom of the Tapeats at lowest falls, Lower Elves Chasm. Purple layers (white arrows) with nearest layers at lower right, typically 3–16 cm thick.

light rock to the left of the falls. However, an additional tapering of many bedding planes can be seen within the near layers on the right. These are low-angle foreset bedding planes that McKee et al (1967) and Barnhart (2011b) determined to indicate decreasing velocity. They suggest the increasing mixing of ambient water with the debris flow and would appear as the plastic flow transitions to a more fluidal flow.

Figure 10 illustrates the bedding near the water level at the base of the falls in Figure 12. The irregular layering of purple and white laminae is typical of hyperconcentrated laminar bedforms. Thus, it appears that all of these sediments were deposited from a plastic flow throughout the section visible in Figure 12. This suggests rapid deposition with another regular overlying energy pattern.

Figure 13, at Red Canyon, is at or near the top of the Tapeats—the transition zone of McKee (1945). Individual layers are approximately the same thickness as those at lower Elves Chasm falls (Figure 12). Though this pattern is not constant through the entire thickness of the Tapeats, the next paper in this series will argue that depositional conditions were similar throughout. The ubiquitous purple sand can be seen here as a dark streak across the large rectangular block just right of lower center and as the dark layer between lighter layers in the overhanging ledge above the block's far end.

About 7 km further west at Blacktail Canyon is another exposure of the basal Tapeats at the Great Unconformity. In Figure 14 a clast of rounded quartz is suspended in a sand matrix to the right of the image. The clast's position indicates plastic behavior in a sandy debris flow (Figure 5). This is contrary to the quiet tidal environment posited by many geologists. In a fluvial or marine tidal setting, the sediment would have been carried in water with a low concentration of solids and with no dispersive shear stress; thus, the most prominent stress on the quartz clast would have been from traction in the bedload. Finer grains would have been carried higher in the suspended load over the saltating larger clasts. In that case, saltation and rolling would have continued until local traction stress halted the progress, most likely in a small cluster of grains. In this case, the clast would have been deposited with its longest axis, d_A, perpendicular to flow. A rolling cobble naturally turns its intermediate and short axes, d_B and d_C respectively, parallel to flow to facilitate rolling with minimal energy expended (Smith, 1986). Since d_A is parallel to flow, the quartz was suspended in a matrix with d_C perpendicular to flow, again following the least resistance. Suspending a cobble of this size would require a viscosity higher than water; it would require plastic flow. If the bedforms were deposited in a plastic debris flow, then what was the current velocity?

Velocity of the Basal Tapeats

The floating quartz clast in Figure 14 allows a minimum velocity calculation for the flow depositing the basal Tapeats. It is the minimum because a higher velocity would entrain the clast. Scale is uncertain in this photo, but using a length of 7 cm for the index finger, the quartz is 3.8 x 7.7 cm, and the layer is

Figure 13. Laminar layers near the top of the Tapeats, Red Canyon, typical of exposures in the eastern Grand Canyon. Eroded alcove about 1 m high, with typical layers 3–16 cm thick. Some purple layers marked by arrows.

Figure 14. Contact of basal Tapeats Sandstone at Great Unconformity with gneiss below. Quartz clast is about 3.8 x 7.7 cm in the middle of a 10.5 cm layer. From area of Blacktail Canyon. Modified from http://www.thegreatstory.org/great-unconformity.html (accessed December 2010).

10.5 cm thick. For these hydrodynamic calculations, the following symbols will be used:

γ_s = specific gravity of the solid phase

γ_m = specific gravity of the water/solid mixture based on the percent concentration of solids

d = diameter of the sediment particles

τ = total shear stress

τ_* = dimensionless shear stress for the solid particles

τ_o = critical shear stress for initiating particle motion

h = flow depth

S = slope steepness factor

f = friction factor

μ = dynamic viscosity of water

μ_m = change in dynamic viscosity for mixture

V_o = critical velocity initiating particle motion

$\overline{V}$ = depth averaged flow velocity

Fr = Froude number

e = natural log

The critical shear stress (τ_o) can be determined from the Shields equation (Julien, 1998):

$$\tau_o = \tau_* (\gamma_s - \gamma_m) d_{max} \quad (1)$$

Julien (1998) gives τ_* = 0.05 for very coarse gravel (>32 mm), 2.65 g/cm^3 is the density of quartz, and d_{max} = 3.8 cm, the d_B measurement calculated from Figure 14. For a non-Newtonian fluid, Julien (1998) gives the range of 5–60% solids by weight for hyperconcentrated flows. Lowe (1982) preferred a narrower range of 20–30% solids by volume, about 42.1–52.0% by weight (based on Julien's, 1998, p. 174 conversion). To reach a 25% concentration by volume, a 46.9% concentration by weight would be required. The higher concentrations produce lower values for critical shear stress (τ_o), flow depth (h), and velocity (V). Using the analogy of the Katrina splay deposits, I want to compare the two bedforms. Therefore, I am providing parallel calculations with the same 20–30% solids by weight used for the splay deposits. This gives a range of values: τ_o = 21.6 N/m^2 for 30% solids and 24.6 N/m^2 for 20% solids (Table I).

The DuBoys equation (Lalomov, 2007) calculates flow depth (h) from critical shear stress (τ_o):

$$h = \tau_o / \gamma_m S \quad (2)$$

For slope (S), Hereford (1977) provided sedimentary evidence of braided

Table I. Minimum Velocities
calculations based on clast size d_B = 3.8 cm (Figure 14)

τ_* (Pa)	S	density	d_{max}	% solid (vol)	τ_o (Pa)	h (m)	d_{50} (m)	n	$\overline{V}$ (m/s)	Fr	f	V_o (m/s)
0.05	0.0025	2.65 g/cm^3	0.038	20	24.6	0.755	0.0005	0.0175	2.37	0.87	0.0427	0.51
							0.00025	0.0156	2.66	0.98		0.57
				30	21.6	0.590	0.0005	0.0175	2.01	0.83	0.0468	0.52
							0.00025	0.0156	2.26	0.94		0.59

stream deposition for the Tapeats. Schumm and Khan (1972) noted that flume evidence shows that braided streams require a minimum slope of 0.016. Using $S = 0.017$, a flow depth of $h = 0.11$ m, is obtained for flow with 20% solids and $h = 0.087$ m for 30% solids by weight. Because these depths are too shallow to produce layers of 0.105 m, they were not deposited on a slope steep enough for a braided stream.

Another option is found from the work of McKee et al. (1967, p. 839, brackets added) on the Bijou Creek flood deposits. If these were hyperconcentrated flow products (Barnhart, 2011b), "the flooded surface must have been quite irregular, as shown by variations in thickness of sand deposits [his figure 6: (6 - >30 in)] despite a relatively flat, even top." McKee et al. (1967) determined the height of sediment deposited under a wide flooding current was directly related to the elevation of the top of the current, not the variations in the topographic substrate. While they could not or did not determine what the flow depth to sediment height ratio was in the Bijou Creek flood, that calculation in similar situations can help answer the question of depth.

Barnhart (2011b) determined that the Katrina splay deposits exhibited a ratio between depth and bedding thickness of 8:1 to 10:1, and Allen (1976) thought 6:1–8:1 was typical. Based on these values, Equation (2) was solved for slope (S) when $h = 0.63$–1.05 m. The resulting range for the slope was 0.0014 to 0.0030. A median value, $S = 0.0025$, was used. Substituting it back into Equation (2), flow depth would have been in the range of $h = 0.59$–0.76 m (Table I). While there is no physical evidence to determine the actual sub-Tapeats slope, the comparison of these two slopes, 0.017 and 0.0025, shows that a shallow slope better fits the hydraulic data.

The Manning Equation (Julien, 1998) is used to calculate depth-averaged flow velocity ($\overline{V}$):

Figure 15. Detail of Tapeats breccia at Great Unconformity.

$$\overline{V} = S^{1/2}\, h^{2/3}\, n^{-1} \qquad (3)$$

The value of the Manning coefficient (n) for all sizes of sand to fine gravel is $n = 0.02$ (Julien, 1998). He also provided an alternate method of deriving the coefficient directly from the grain size (p. 97) as $n = 0.062\ d_{50}^{1/6}$. This gives $n = 0.0175$ for medium sand (0.0005 m) and $n = 0.01556$ for fine sand (0.00025 m). McKee (1945) identified both in the basal Tapeats. Based on these factors, the basal Tapeats depositional depth-averaged velocity ranged between 2.01 and 2.66 m/s (Table I).

The Froude number is a ratio of the inertial forces to the gravitational forces and is derived from the equation (Julien, 1998, p. 38):

$$\mathrm{Fr} = V\,(gh)^{-1/2} \qquad (4)$$

High-energy flows will move at depths and velocities that approach Fr = 1.0 in order to maximize energy dissipation and sediment transport (Julien, 1998). Grant (1997 p. 349) stated that Fr > 1.0 would occur only for short periods of time without adjusting "the channel hydraulics and bed configuration." Costa (1987) showed that under the very high energy of flash floods, Fr > 1.0. Kennedy (1963, p. 539) defined the critical flow range between Fr = 0.844 and Fr = 1.0. Here, Froude numbers are a means of checking the relationship between h and V, based on the tendency for Fr to approach 1.0. Table I shows Fr = 0.83 to 0.98, within the acceptable range of expected flow.

Table I shows minimum velocities. Maximum velocities are shown in Table II, based on data from Figure 15. Sedimentary features there also show a plastic rheology, with contemporaneous currents interacting to deposit the sediments quite rapidly. Figure 15 shows breccia that was not entrained in the flow but left between the base of the flow and the Great Unconformity. Unlike Figure 3 at Boucher, the breccia was not against a high limiting the current's ability to pick up additional sediments. The flat beds of breccia visible in the next bed up of Figure 16 testify to this. Since the clast in the foreground was not entrained, calculations based on its size will provide maximum possible flow velocity. The two locations (Figures 14 and 15) are about 40 km apart, illustrating the proposed extent of the currents responsible for the basal Tapeats deposition.

Many clasts in Figure 15 are broken or eroded; the marked clast has a $d_B = 0.064$ m (based on a 7-cm index finger).

Table II. Maximum Velocities
calculations based on clast size $d_B = 6.4$ cm (Figure 15)

τ_c (Pa)	S	density	d_{max} (m)	% solid (vol)	τ_0 (Pa)	h (m)	d_{50} (m)	n	$\overline{V}$ (m/s)	Fr	f	V_0 (m/s)
0.05	0.0025	2.65 g/cm³	0.064	20	41.5	1.274	0.0005	0.0175	3.36	0.99	0.0426	0.56
							0.00025	0.0156	3.77	1.11		0.63
				30	36.3	0.991	0.0005	0.0175	2.84	0.91	0.0469	0.55
							0.00025	0.0156	3.19	1.02		0.62

Repeating the calculations for critical shear stress (1), flow depth (2), and velocity (3) yields the results in Table II; slope and the Manning coefficient are the same in both tables. Flow depth for the basal Tapeats thus ranged between 0.59 and 1.27 m, and depth-averaged flow velocity from 2.01–3.77 m/s. The maximum values for depth and velocity yield Froude numbers near unity.

Can we validly analyze flows with plastic rheology with formulas developed for fully turbulent flow? For a plastic flow to move, it must have a shear stress equal to the yield strength (τ_x) plus the dynamic viscosity of the mixture (μ_m). These quantities are dependent on the concentration by volume of the solids (C_v) and do not vary based on the d_{max} of the solids. Therefore, Shield's Equation (1) is not the best formula for this case.

Julien (1998, p. 188) provided a formula for stress (τ) in a plastic flow, where dv_x/dz is the rate of deformation and said to "rarely exceed 100/s" in natural settings (Julien, 1998, p. 120):

$$\tau = \tau_y + \mu_m \, dv_x/dz \qquad (5)$$

For finding the yield strength in sand, Julien (1998, p. 190) devised the following formula from the graph of multiple data sets:

$$\tau_y\,(Pa) = 0.1e^{\,3(Cv\,-\,0.05)} \qquad (6)$$

While the sand portion of his database is sparse, and I prefer a different best-fit line, varying the line does not produce a significantly larger value for the yield strength. In sand, the formula produces $\tau_y = 1.05$ *Pa* for 20% solids and $\tau_y = 2.39$ *Pa* for 30% solids (Table III).

For finding the change in dynamic viscosity (μ_m) of the mixture, Julien (1998, p. 190) recommended for sand:

$$\mu_m = \mu(1 + 2.5\,C_v + e^{\,10(Cv\,-\,0.05)}) \qquad (7)$$

Table III. Shear Stress Plastic Flow

C_v % solids	t_y (*Pa*)	μ_m (*Pa*)	t (*Pa*)
20	0.157	0.00889	1.05
30	0.212	0.0218	2.39

Calculated results of equations (5), (6), and (7)

This produces values of $\mu_m = 0.00889$ *Pa* for 20% solids and 0.0218 *Pa* for 30% solids (Table III). Even when a maximum value of dv_x/dz = 100/s is used, together these values in formula (5) give τ = 1.05 *Pa* for 20% and 2.39 *Pa* for 30% (Table III). These values are a full order of magnitude smaller than the τ_o calculated form turbulency formulas based on clast size in Table I. In a sandy debris flow, the shear stress can be measured by the yield strength (τ_y), and the dynamic viscosity of the mixture (μ_m) may have little to do with the shear stress needed to entrain larger clasts in the flow. Of course, the energy needed to start flow may be much greater than the yield strength. This extra energy becomes concentrated in the turbulent head and upper surface of the flow (Figure 8.2). This suggests our mathematical understanding of plastic flow is still incomplete when working with sand at the high levels of energy exhibited in the Tapeats Sandstone.

A second way to evaluate the results of calculations in Tables I and II is to compare the velocities obtained with the known critical velocity needed to move clasts of known d_{max} from experimental data. Berthault (2004) cites Lischtvan-Lebediev (1959), who charted the critical velocity (V_0) for many clast sizes at multiple flow depths. A small part of this chart is reproduced in Table IV.

For a comparison with the calculations of depth-averaged velocity ($\overline{V}$) in Tables I and II, critical velocity (V_0) can be calculated by the formulae provided in Rubin and McCulloch (1980, p. 217) based on Keulegan's (1938) classic work:

Figure 16.1. Tapeats Sandstone at Great Unconformity, possibly at Pipe Creek.

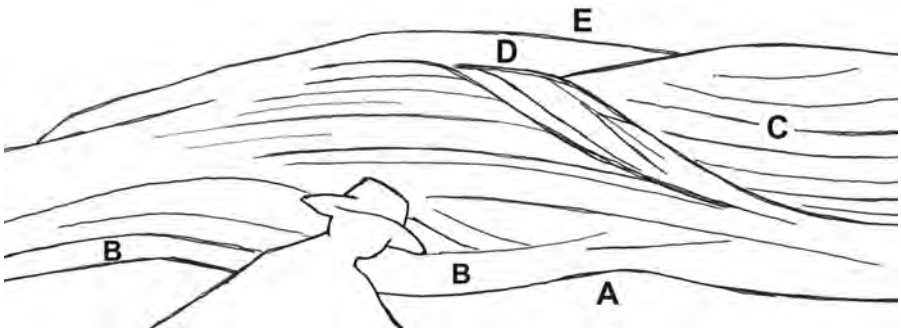

Figure 16.2. Sketch of Figure 16.1 showing: (A) breccia layer with sand matrix at unconformity, (B) traction layer of fine sand, (C) cross bedding of medium to coarse sand, (D) upper breccia layer conformed to uneroded rolling top of cross bedding, and (E) laminar bedded breccia grading into sand.

$$V_0 = \overline{V}\ (5.75 \log (0.37\ h/f))^{-1} \quad (8)$$

The additional variable (f) is a friction factor and Keulegan's (Lalomov 2007, p. 276) is provided as:

$$f = (2.03 \log (12.2\ h/d_{max}))^{-2} \quad (9)$$

Friction factors (f) from 0.0426–0.0428 are calculated (Tables I and II) and produce critical velocities (V_0) with formula (8) from V_0 = 0.51 - 0.63 m/s.

Table IV shows the comparison of Lischtvan-Lebediev's (1959) results with the calculations from Table I for minimum velocities. With allowances made for differences in flow depth and percent concentration of solids, the results from Table I correspond well with the rest of the sequence. This provides confidence that both depth (h) and depth-averaged velocity ($\overline{V}$) as calculated in this paper are realistically in agreement with modern measured data. While the equations for plastic flow may not give us any more information about what is taking place behind the fully turbulent head of the high-density turbulent flow (Figure 8.2), the head is acting in complete accordance with other fully turbulent flows.

Table IV. Critical Velocities Compared

		DEPTH (m)			
		A	B	C	D
% solids	d (mm)	**0.40**	**0.59**	**0.76**	**1.0**
	0.05	0.20			0.30
	0.25	0.35			0.45
20	0.25			0.51	
30	0.25		0.52		
20	0.5			0.57	
30	0.5		0.59		
	1.0	0.50			0.60
	2.5	0.65			0.75

Columns A & D from Lischtvan-Lebediev (1959); concentrations of solids not specified
Columns B & C from this paper (Table I)

Smith (1986) noted that the presence of cobbles in the same flow with sand demonstrates enough kinetic energy to carry the fine sand in suspension; at sufficient concentrations, the entrained sand would dramatically affect fluid viscosity and carrying capacity. Thus, conditions for the basal Tapeats may well have been close to the maximum values of Table II. Keeping Fr close to 1.0 provides a check on any set of conditions.

But why was the fine sand of the traction layer not eroded by these high velocities? One answer is that deposition occurred from a hyperconcentrated flow, under plastic conditions behind the turbulent head, in a unidirectional current overlaid by energy pulses, such as would be expected from storm waves. Figure 8 illustrates this type of current. Figure 8.1 shows that the only part of such a current where turbulence contacts the substrate is at the turbulent head. Behind it, laminar flow at the substrate/current interface shields the substrate. Because all of the water is moving as a part of a continuous current, a second and third wave of bedforms (Figure 8.3) would override the first, leaving additional layers while not exposing the substrate to additional turbulence from the current's head.

If distinct layers were deposited by pulses of energy or sediment, what caused these pulses? Foley and Vanoni (1977) described how bore waves are generated by the continual breaking of standing waves and the release of stored water from them at certain conditions of shallow flow depth and velocities close to critical. These standing waves are generated by growing antidunes beneath them. Bore wave periods vary from 44 sec at 0.471 m/s to 7.8 sec at 0.275 m/s (Foley and Vanoni, 1977).

Julien (1998) speculated that at Fr = 1, wave celerity should equal current velocity, causing wave and current to travel synchronously. It seems apparent that he is referring to deepwater waves. Deepwater waves are limited by flow velocity, which breaks them into multiple shallow waves (Barnhart, 2011b). Dispersal pressure acts on an isolated wave front (McLane, 1995), breaking a single wave into multiple waves. It follows that a current can also be broken into multiple energy wave fronts. Storm waves superimposed on a current can produce such pulses. Where there is a flux in current energy that changes the elevation of the flow surface, such as bore waves cited by Foley and Vanoni (1977), there is a corresponding change in the thickness of the boundary layer (Ippen, 1951). Such a rise in the boundary layer will produce a change in pressure at that point in the flow; this could be the initiating factor for a new layer of sediment.

Smith (1986) in the Neogene Deschutes Formation, central Oregon, and Sohn et al. (2002) in the Cretaceous Cerros Toro Formation, Southern Chile, both document rheologic changes from a subaqueous debris flow to a hyperconcentrated flow producing laminar

bedforms caused by dilution of the flow (Figures 8.3 and 8.4), extending over 10's of km. Lamb et al. (2010, p. 1070) note that hyperpycnal flows (high-density turbidity currents under ambient water) remain coherent for extended periods after plunging and can experience "multiple acceleration and deceleration … due to the intrinsic phenomenon of plunge point translation for even the most simple flood hydrograph and bed topography." Sohn et al. (2002) provide a model for multiphase or pulsating forms of these flows (Figures 8.3 and 8.4) as they divide and/or hydroplane as a result of the additional entrained water.

What was the period of these bedforms that compose the basal Tapeats? While calculations (Table I) suggest fairly shallow flow, under 1.5 m, the period of shallow water waves is too low. While they may have influenced deposition higher in the formation when flow became less plastic, the depositional current requires longer waves. McLane (1995, p. 72) suggested a storm wavelength of 600 m would have a period of about 20 seconds. Because these are fairly thick layers, the wavelength may need to be even longer. A wavelength of 1000–1200 m would result in a period of about 40 seconds. Based on a mean layer thickness of 10 cm and on each layer being deposited by a storm wave, sedimentation would proceed at a rate of 1 m every 400 sec or 0.15 m/minute. If single wave fronts divided into multiple waves, creating the possibility of overlying patterns of shallow water waves, this rate could be even faster. Katrina splay deposits showed six recognizable wave crests from each deepwater wave. This would produce a sedimentation rate of an amazing 0.9 m/minute.

Trough Cross Bedding and Debris Flows

Hereford (1977, p. 206) described various facies of the Tapeats in the Chino Valley area of central Arizona (Figure 2). His "facies C," in the basal Tapeats, was characterized as: "low (2°–10°) to medium (10°–20°) cross-stratified, trough cross-stratified tangential foresets, no alternation of coarse-fine foresets." McKee (1945) identified trough cross bedding cut into flat beds of the basal Tapeats in the eastern Grand Canyon. Rose (2006, p. 228) may have called the same feature "amalgamated channels of tangentially cross-bedded arkosic to subarkosic coarse to very coarse to gravelly sandstone." Though cogent, he was describing rocks higher up in the Tapeats Formation.

It is worth reexamining McKee's (1945) "trough cross bedding," which he documented at four locations (Figure 17), noting the angles of repose of 23° and 27°. Since these angles correspond to the erosion surface and are not the same through the thickness of the deposit, had the erosion scoured less, the angles also would have been less and would have matched more closely the 2°-20° Hereford (1977) recorded in central Arizona. McKee's (1945) four locations are relatively grouped and are all adjacent to monadnocks. He identifies the bedforms at each one as "scour and fill structures" (p. 43). McKee (1945) interpreted the features as bedding created by migrating sand dunes filling channels previously cut by accelerated currents. That is the common explanation of trough cross bedding (McLane, 1995; Nichols, 1999). However, McKee (1945) failed to notice several subtle differences in the Tapeats cross beds and later discovered (at Bijou Creek) that flooding bedforms can be "similar to the type commonly ascribed to intermittent accumulation" (McKee et al., 1967, p. 850).

Scour and fill and trough cross bedding are now seen as two different bedforms. Figure 18 shows both bedforms in a block diagram. While perpendicular to flow, scour shows tangential contact of the leading edge of each foreset and occurs en echelon when viewed parallel to flow. Cut and fill, by contrast, exhibits primarily parallel bedding planes, parallel to flow and with the likelihood of tangential contact along the edges of the cut channel only. Additionally, larger clasts may be found along the bottom edges of the cut channel, where they were left as lag from the scouring process having been moved as bed load.

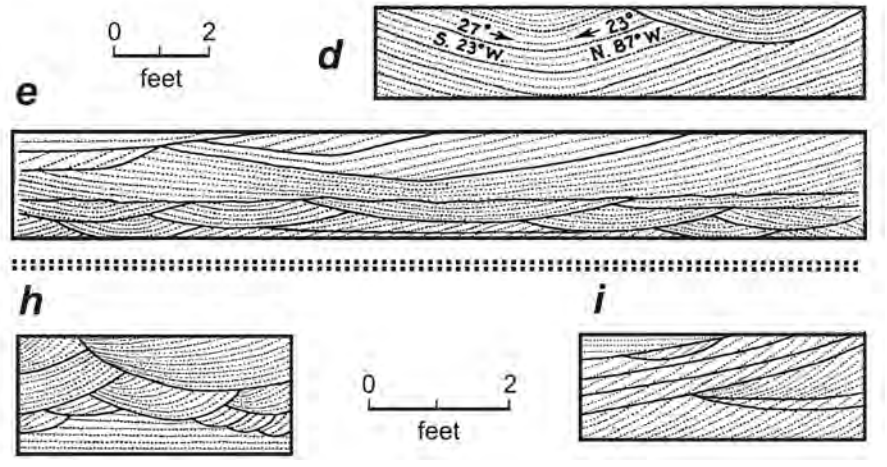

Figure 17. Lamination patterns in Tapeats Sandstone beds. From figure 5 in McKee (1945). d = East fork, Pipe Creek; e = East of Pipe Creek; h = Near Yaki [now South Kaibab] trail; i = West Fork, Pipe Creek.

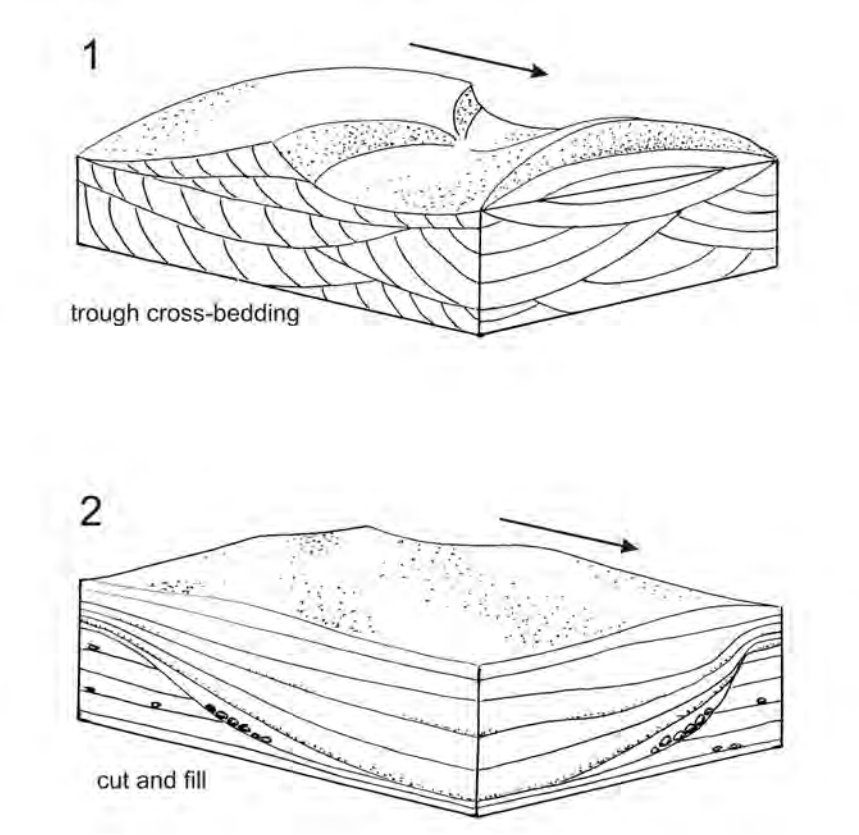

Figure 18. Block diagram. (1) Trough cross bedding (after Nichols, 1999, his figure 4.11); (2) cut and fill bedding.

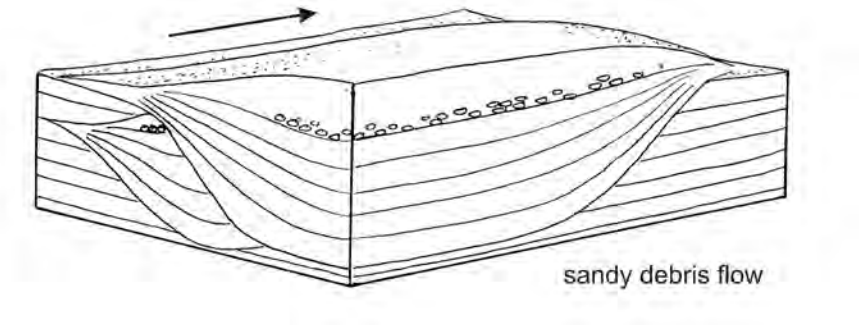

Figure 19. Block diagram of sandy debris flow deposits.

Sandy debris flow (Figure 19), by contrast, will show parallel bedding planes both perpendicular and parallel to flow, with larger clasts suspended at the top of the deposits where they were carried, rafted on the top of the hyperconcentrated laminar bedforms. Additionally, debris flow will show characteristics of sediment layers typical of plastic flow, while scour and fill or trough cross bedding may be plastic or fluidal.

The cross bedding perpendicular to flow in a sandy debris flow shows the bottom layer to lie perfectly cupped in the eroded channel. This is too accurate a fit to have been accomplished by one wave or current eroding the scour and a separate current with a slightly varied direction of flow depositing the first layer. Figure 20 shows dunes, even 3D dunes, are consistently deposited at a lower velocity for all grain sizes than high-velocity flat beds. If the flat beds show characteristics of deposition by high-velocity currents, as I have shown the lower Tapeats to be, then dune formation, according to Figure 20, would indicate a sharp decrease in velocity that would not erode down into a bed laid at a higher velocity.

McKee (1945, p. 41) noted a "considerable contrast in the average grain size of adjoining laminae." This implies the layers are discernible by grain size, but a careful look at Figure 21, the deposit with the clearest image of these features, shows that the layers are not as clearly discernable as those often seen in cross bedding. Instead, they are reminiscent of hyperconcentrated laminar bedforms from flood flows in the debris fields of Mount St. Helens (Figure 9) or those at Bijou Creek. The small flow of Figure 21.1, located along the Kaibab Trail (Figure 7), corresponds to McKee's (1945) figure 17h. The top exhibits "outsized rafted clasts." That is a characteristic of debris flows (Figure 5.1), but these are no larger than small pebbles and coarse sand. However, in this case that is likely a factor of sediment source rather than velocity. These clasts were the largest available of the entrained sediments and dispersive shear pushed them to the top (Figure 5.2).

Trough cross bedding typically forms in fluidal conditions, where turbulence keeps particles in suspension that settle out at a constant rate while the flow

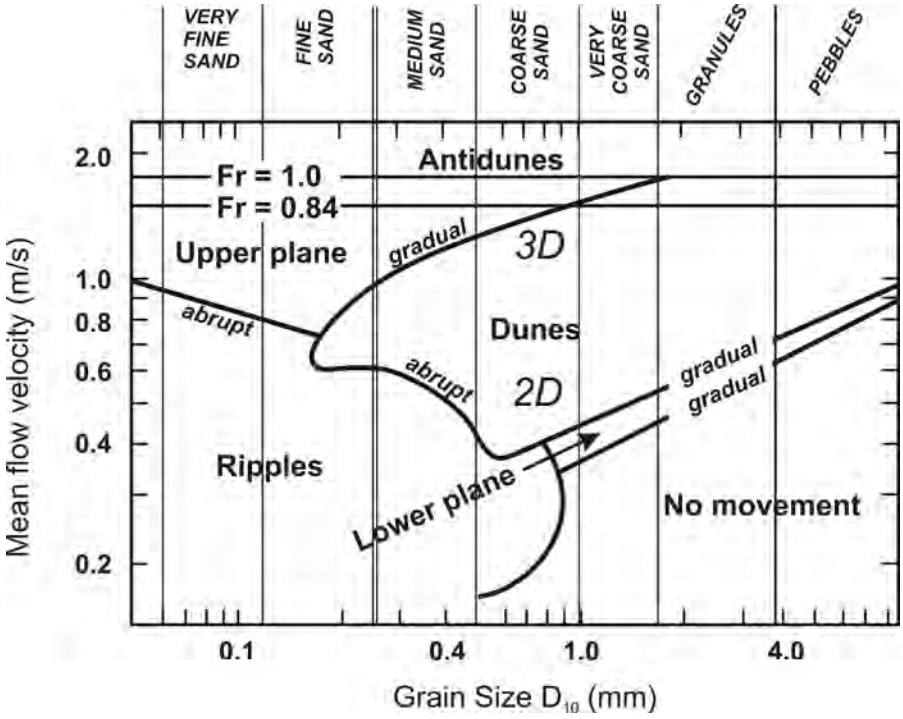

Figure 20. Bedform stability fields by grain size divisions, showing the bedform progression for velocity increase and decrease. After figure 5.15 in McLane (1995).

moves the bedload. They are deposited grain by grain as they cascade down the lee slope of a dune (Julien et al., 1994). In contrast, the Tapeats layers here appear to have been deposited under plastic flow conditions.

Figure 22 is a sketch made from the photograph of a very thick volcanic debris-flow conglomerate in the Laguna Goth section of the Cretaceous Cerro Toro Formation in southern Chile (Sohn et al., 2002). It, too, shows incision into flat beds, irregular discontinuous layers of sediment parallel to the erosional surface, erratic wandering of the current eroding into previously deposited materials, and a coarse sediment cap in the central area of each individual flow. These are similar to features of the "trough cross bedding" or "scour and fill" found in the Tapeats. Since the Cerro Toro deposits are considered debris flow sediments, then these similarities suggest the same origin for these deposits in the basal Tapeats.

Shanmugam (1996, p. 2) classified a debris flow composed primarily of sand as a "sandy debris flow," and he would use the term to replace "high-concentration turbidity flows" and "mass flows" commonly seen in the literature because the plastic flows do not involve flow turbulence in the depositional layer. He cited Dott's (1963) definition of a mass flow as being most descriptive:

> (1) A "non-Newtonian flow that exhibits plastic behavior." (2) High concentrations of sediment supported by "dispersive pressure (caused by grain collision), hindered settling, and buoyant lift (caused by mixture of water and fine grains) (modified by Postma et al., 1988)." (3) "Deposition from these flows occurs by 'freezing'" (Shanmugam, 1996, p. 7).

While Shanmugam (1996) provided no cross-sectional diagram of a sandy debris flow, Figures 5.1 and 5.2 are based on his figures of a "high-density turbidity current" deposit with larger clast sizes.

Furthermore, the "trough cross beds" in the Tapeats never pinch out to form tangential foresets at either end. What appear at first glance as tangential ends are in fact erosion surfaces cut by an erratically wandering current. Sedimentary layers are produced by laminar flow at the bottom of the high-concentration turbidity current (Figure 8.2), leaving irregular alternations of coarse and fine sediments as predicted by Figure 5.2. These are frozen as one body when the shear stress declines sufficiently. Each new trough in the stack begins with a new tongue of the flow preceded by its own "flow front [that] can be repetitively detached and diluted to form voluminous turbidity currents. The turbidity currents outpace or are outrun by the debris flows resulting in extensive turbidites beneath and above the parental debris flow deposits" (Sohn, 2000, brackets added). While I would side with Shanmugam (1996) in not using the term "turbidites," Sohn (2000) and Sohn et al. (2002) are still referring to the same bedforms that originate from a sandy debris flow. Within a debris flow current, there would be multiple tongues, some with their own turbulent head. These would erode into previous deposits and leave multiple layers of sediment, some with laminar flow layers and some with irregular discontinuous layers. The sedimentation style would depend on the extent of dilution of the debris flow at the time of deposition, but each of the layers deposited behind the turbulent head will be laid down roughly parallel to the original eroded channel surface (Figure 19).

Figure 16 shows the lowest occurrence of a sandy debris flow, immediately overlying the Great Unconformity. It matches the pattern of McKee's (1945) figure 17d, located on the east fork of

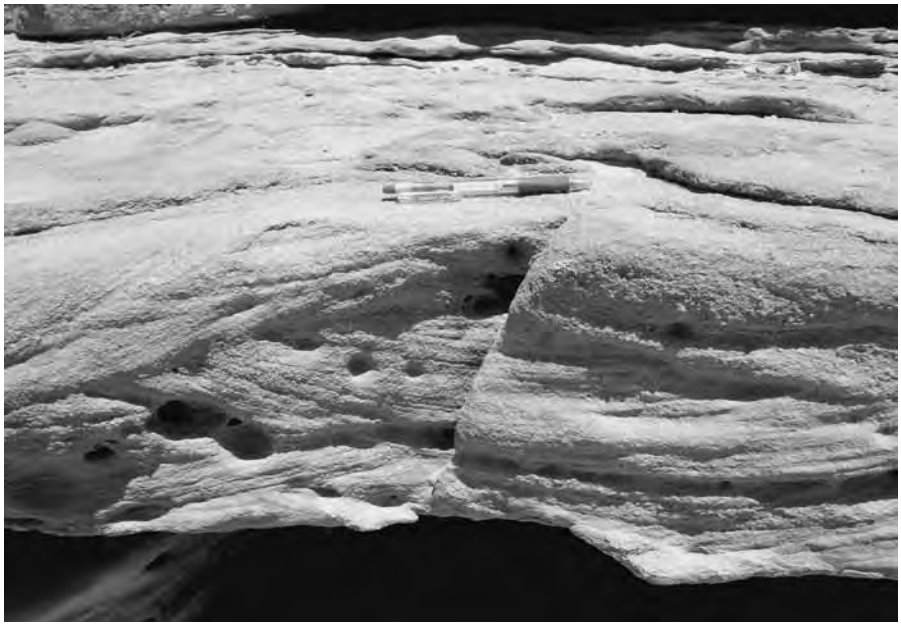

Figure 21.1. Trough cross bedding in Tapeats Sandstone, South Kaibab Trail (Yaki Trail of McKee, 1945). Photo from Oard (2010).

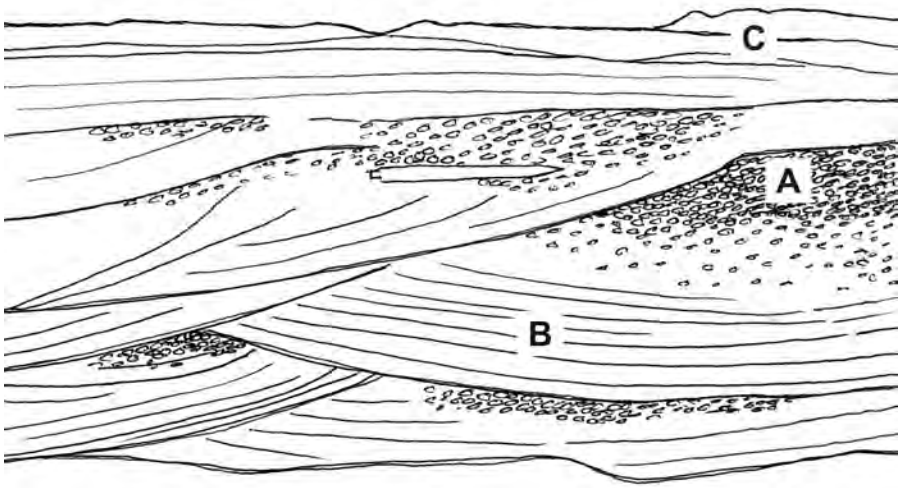

Figure 21.2. Sketch showing (A) disorganized outsized rafted clasts of coarse sand, (B) general trend of trough cross bedding, and (C) hyperconcentrated laminar bedform.

Figure 22. Sketch of trough cross bedding in Laguna Goth section of volcanic debris flow, taken from a photo. Paleoflow direction is to the left and obliquely into the page (arrow, lower left). Scale is about 8 m at A. Based on figure 4 in Sohn et al. (2002).

Pipe Creek (Figure 7). This occurrence is the only example in this study where a debris flow did not erode underlying high-velocity flat beds or it eroded them all the way down to the crystalline basement. It is composed of mature, well-sorted fine sand. Lowe (1982) recognized the traction layer (his layer S) as the lowest division of a sandy debris flow (Figure 5.2). The flat beds of breccia, visible above the sandy debris flow of Figure 16, show that either the cascading of breccia down paleotopographic highs was a recurring event or that the debris flow occurred during such a cascade. Conglomeratic high-velocity flat beds directly above high-velocity flat beds illustrate the debris flow was part of a larger energetic event, not an isolated energy pulse.

If the majority of the basal Tapeats is formed of hyperconcentrated laminar layers, irregularly interrupted by interspersed debris flows (apparently associated with monadnocks), then this mechanism of cascading clasts off monadnocks may account for the infrequent gravity flows. Flat beds of breccia in the background of Figure 16.1 support this mechanism as the energy source behind the debris flow as it descended and pushed the previously settled sand ahead of it as a plastic flow. Both Scott et al (1995) and Smith (1987) cite sidewall failures in volcaniclastics that were previously in stable equilibrium as the most common source of gravity flows off areas of volcanic debris.

Figure 11 shows a thick section of sandy debris flow that matches the pattern of McKee's (1945), figure 17e, east of Pipe Creek (Figure 7). The photo was labeled "Peach Springs Canyon," and the location is uncertain. It shows angular foresets, bounded below and above, by hyperconcentrated laminar bedforms. This arrangement is also seen in Figures 3 and 4. Bedforms comprised of a mixture of purple and white sand (Figure 10) also suggest that the debris flow was just a part of a more extensive

high-velocity flooding event. Combined with the high-velocity flat beds of Figure 16, we see that all the layers of the basal Tapeats were deposited during a continuing unidirectional current covering a large area.

Chadwick and Kennedy (2001) provided one photo and measurement of what is possibly the largest breccia deposit yet documented alongside a monadnock. Found in 91 Mile Canyon (Figure 7):

> The breccia underlies most of the Tapeats Sandstone as well as 112' of Bright Angel Shale along the Precambrian slope. Breccia extends for vertical distances of up to 140 meters and horizontally up to 2 kilometers from the Shinumo outcrops … exhibiting no evidence of post-depositional erosion or reworking prior to burial. The breccia persists up-section, along the Precambrian contact, in some cases underlying the entire thickness of the Tapeats Sandstone and portions of the Bright Angel Shale. (Chadwick and Kennedy, 2001, p. 3)

The height of this breccia slide is Chadwick and Kennedy's (2001) primary evidence for their proposed water depth of > 200 m. Their use of the phrase, "in some cases," suggests that some intertonguing of the breccia flow may occur with the Tapeats or Bright Angel and would thus make 91 Mile Canyon a very profitable research location to document the specific interactions of the Tapeats, Bright Angel, and breccia to help determine the energy profile of the depositing event.

Rose (2006) documented another debris field of breccia in the vicinity of Zoroaster Canyon (Figure 7). The debris flow sediments persist up to the transition zone between the Tapeats Sandstone and the Bright Angel Shale. Boulders of Precambrian Zoroaster Granite lay next to a monadnock of the same composition. This is the largest breccia deposit documented at this stratigraphic level, and does not appear to be connected with stratigraphically lower flows. However, it does shed light on the energy of events throughout Tapeats deposition; the entire formation may well be the product of a single event, not different events separated by long periods of time. It may also suggest increasing energy conditions persisting even near the end of sandstone deposition and the transition to clay and mudstone in the shale above. If so, it would be contrary to most interpretations of the transition from the Tapeats to the Bright Angel.

Discussion

Sedimentology

Contrary to the proposed facies models of most geologists, this sedimentological analysis of the basal Tapeats demonstrates deposition by energetic events, leading to debris flows, breccia cascades, and hyperconcentrated laminar bedforms. Whether such events represent the regressive current that might have eroded the Great Unconformity in its transgressive phase, as Berthault (2004) described, it is unlikely that the unconformity surface was exposed for any significant time period as a subariel surface. Weathering, identified by Sharp (1940), was used by others (McKee,1945, Hereford, 1977, Rose, 2006) to posit an extended period of exposure for the unconformity prior to the start of sandstone deposition. Up to 1.2 Ga (Karlstrom et al., 2003) is supposed to be represented by the contact between the Vishnu Schist and the Tapeats.

This "weathering" was recently attributed by Rose (2006) to redox processes. While some occurrences of this bleaching are restricted to surfaces below the unconformity, like the Hakatai Shale (Figure 23) below the erosion surface on the monadnock, and might have been produced by chemical weathering while exposed during the 1.2 Ga hiatus, other locations, such as one along the Clear Creek Trail (Figure 4), show bleaching

Figure 23. Great Unconformity in Garnet area with a Precambrian high of liver-red Hakatai Shale cut by a basalt dike. Tapeats Sandstone on right abuts Hakatai without any "run up" (lower arrow). Bleaching occurs on upper ridge of Hakatai from dike to the top of the high (upper arrow). Distance from river to the bottom of the dike, at its upper end, is about 10 m.

extending up from the Vishnu Schist into the sandstone. Rose (2006) thought that oxidizing pore fluids in the Bright Angel Shale produced similar results. If bleaching in the Bright Angel was the result of diagenesis, then it is reasonable to suspect that might also be the case in the Tapeats. Figure 4 shows a cavity that seems to be the locus of bleaching that spread outward across the unconformity. The bleaching extends an equal distance in all directions, even across the supposed 1.2 Ga unconformity (Barnhart, 2011a). This juxtaposition of ripple bedforms, sandstone deposition, and bleaching shows that these were not events separated by millions of years. If so, the time thought to be present in the unconformity surface as well as that thought necessary to produce the "facies" of the Tapeats may not be necessary to explain the field evidence.

Another "evidence" for extreme age is the use of the term "regolith" for the breccia deposits in the basal Tapeats.

> Distinction between sedimentary source and basin are obscured in low-relief, low-slope cratonic interiors; the bulk of sedimentary cover in such settings must therefore be seen as resident regolith. (Rose, 2006, p. 234).

This conclusion rests mainly on the assumption of long periods of time, not field evidence. As such, the conclusion is circular. The presence or absence of weathering in the basal Tapeats or along its subcrop is something to be demonstrated. The breccia clasts do not appear weathered. They are not a part of a paleosol (Klevberg et al., 2009), as would be expected if subaerially exposed, and there are few, if any, attached invertebrates to suggest an ancient beach. The petrology and position of the cobbles and boulders indicate an origin atop adjacent elevations, suggesting only that they were broken or eroded from those highs, and then tumbled downhill under the influence of the current and/or waves that deposited the basal Tapeats.

Rose (2006, p. 228) described the Great Unconformity in the eastern Grand Canyon, where the monadnocks occur, as a "peneplain with only local relief in excess of a few meters per 100 meters laterally." So other than occasional monadnocks—including one that reached 140 m above the surrounding surface at 91 Mile Canyon (Chadwick and Kennedy, 2001)—any violent transgression across the areas would have met comparatively little topographic resistance.

The Tapeats Sandstone has long been interpreted within the framework of uniformitarianism. As far back as 1795, James Hutton proclaimed, "The past history of our globe must be explained by what can be seen to be happening now.... No powers are to be employed that are not natural to the globe, no action to be admitted except those of which we know the principle" (Hutton, 1795, cited in Holmes, 1965, p. 43).

Three conditions are stipulated here, and for a mechanism of erosion or sedimentation to be acceptable it needs to satisfy all three of them.

1. "Can be seen to be happening now." While this point is often viewed by most casual observers as the most important, it does not stand alone. Hutton tied it to the following two conditions.
2. "Power must be natural." But this also implies the power must be adequate. McKee's (1967, p. 850, brackets added) statement relates here: flood sediments (high energy) are very "similar to the type commonly ascribed to intermittent accumulation in quiet water [low energy] over a long period." There is a large difference between low energy operating over a long time and high energy over a short time. There are "natural" conditions for both possibilities.
3. "Know the principles." The principles of erosion and sedimentation are becoming better defined empirically, but geologists must be certain that they understand and apply them in proportion to the power exhibited in the nuances of the bedform. This is where the facies model approach fails. While a given modern environment may satisfy some observations and appear to be a shortcut to a fuller understanding of others, a more careful observation and measurement of those conditions may show power and principles outside the possibilities of that facies.

The Flood is often viewed as a cause for erosion and sedimentation outside what "can be seen to be happening now" and therefore violates Hutton's first condition. It is a mistake to view the Flood as a giant facies model; that approach has proven much less profitable than hydrodynamics. Though the Flood was outside of modern experience, flooding is a regular, observed occurrence, and its principles are increasingly well understood through the discipline of fluid dynamics, which applies to a variety of media over a variety of scales, from micrometers to kilometers (Marusic et al., 2010; Rubin and McCulloch, 1980). Therefore, with more complete understanding of these physical principles, explanatory solutions to *geological* mechanisms of erosion and sedimentation at appropriate scale may be achievable.

McKee (1945) tried to satisfy the first of Hutton's points by proposing a long, slow transgression to account for the Tapeats exposures. He limited the portion involved at any one time by positing the slow continual advance of the shoreline. The areal extent of the Tapeats is still problematic, given the scale of modern marine incursions. To account for this, Rose (2006) made much of the differences between the Tapeats associated with the monadnocks in the eastern

canyon and that covering the level peneplain in the western canyon. He emphasized that no actual bedding plane or fossil assemblage can be physically traced from the western to the eastern exposure. Despite the implication, he never came out and said that the Tapeats is not a continuous formation.

Hereford (1977) traced the formation an additional 230 km south to near Payson (Figure 7). In central Arizona, Hereford (1977) located monadnocks in the areas of St. Matthews, Hickey Mountain, northwest of Cherry, and west of the Big Black Mesa. He correlates his facies C, in central Arizona, with McKee's (1945) descriptions of the Tapeats in the Bright Angel Creek area (the area of monadnocks and sandy debris flows). Hereford's noting monadnocks running north to south emphasizes the similarities of the Tapeats subcrop and by implication the Tapeats deposition. Using these authors' descriptions to draw a rough triangle, the minimum area of the Tapeats is about 23,000 km^2. To account for this large area, Hereford (1977) split the Tapeats into six facies—from onshore to shoreline to offshore. Hereford (1977, p. 204) pointed out, "Sedimentary structures in faces C … are common in modern beach environments." And, his model "assumes that in the western half of central Arizona the Tapeats Sandstone was deposited primarily on sandy intertidal flats where the rise and fall of the tides molded the coarse sediments into many different forms" (Hereford, 1977, p. 209). But he would have done well to heed McKee et al.'s (1967, p. 850) caution: "Much of the layering is in the form of fine laminae similar to the type commonly ascribed to intermittent accumulation in quiet water over a long period of time."

Hutton's first point is largely rejected by geologists today. The Tapeats simply adds another reason. Does attributing the basal Tapeats to debris and hyperconcentrated flows find modern analogs, things that "can be seen to be happening now"? It certainly does help us identify an "action … of which we know the principle." I have correlated Tapeats bedforms with those from flooding associated with volcanism. But they do not approach the size of the Tapeats. What are the most common occurrences of these flows today?

The most cited occurrences for debris and hyperconcentrated flows are in overbank splay deposits and alluvial fan deposits (Smith, 1986), fluvial fan deposits, and proximal submarine fans with subaqueous sediment gravity flows (Balance, 1984). Smith (1986) recognized that any such flows deposited by fluvial processes are seldom more than 10 km in radius, while volcanic "debris flows may extend 100 km or more from their sources … and combined with high-sediment loads, may construct aprons of coarse volcaniclastics debris covering hundreds of square kilometers" (Smith, 1986, p. 1). If we are seeking a modern analog, the volcanic model seems the only one that could possibly result in a deposit the size of the Tapeats.

Subaqueous gravity flows down canyons do cover large areas of the ocean floor, but these are not good analogs for the Tapeats. The erosion surface of the Great Unconformity is a peneplain projected to extend many hundreds of km, both to the northeast, the direction of the sediment source, and the west, the direction of transport (Rose, 2006). It provides no elevation or erosional features at its perimeter high enough or large enough to produce such a gravity flow that is comparable to canyons off the edge of today's continental shelf.

What about storms and hurricanes? Unfortunately, they do not generate plastic flows that deposit sediments exceeding 10 m in thickness. This paper has documented those kinds of flooding events to have occurred from the start of deposition (Figures 3 and 16) and to continue well up in the deposits (Figures 11 and 12). It is possible that these various layers represent multiple storm events, but the layers in between, like those in Hurricane Katrina splay deposits (Barnhart, 2011b, his figure 5), show no visible break with layers at the top genetically connected to layers at the bottom (Figure 13). This connection through the middle and upper Tapeats will be the thrust of the final paper in this series. All evidence seen here requires a continuously depositing, essentially unidirectional current during the entire period of deposition. Furthermore, no modern beaches or estuaries cover the area of the Tapeats. Comparisons of this sort are speculative and not well supported by evidence. Attributing the differences to the lack of vegetation (another uniformitarian speculation) per Hereford (1977) or an expansive epicratonic estuary (Rose, 2006) is simply an admission that the Tapeats is not like modern deposits and thus, like so many other features of the rock record, runs counter to Hutton's dictum.

Hydrodynamics

How reasonable are the velocities as calculated in Tables I and II? Costa (1987) correlated data on the twelve largest flash floods in small basins—0.39 to 368 km^2—much smaller than the Tapeats depositional area. Costa's (1987) work showed velocities of 3.47 m/s to 9.92 m/s. These are significantly higher than those in Tables I and II. While slopes on Costa's flood surfaces varied from 0.000286 to 0.0964, his correlation between slope and velocity was weak. Froude numbers varied from 0.81 to 2.49. Like velocity, his Froude numbers did not correlate well to slope; the lowest Froude numbers do occur with the lowest slope ratio.

Costa's (1987) relationships between different parameters suggest some value in varying those in Tables I and II to see how velocity varies (Table V). A flow depth of 1.05 m was obtained for the 10:1 ratio of flow depth to bedform height. Equation (2) thus yields a slope of 0.0014, a value well within the pos-

Table V. Revised Velocities
Calculations based on lower slopes and increased flow depth (h).
Set of velocities obtained by increasing Froude number to 1.2

S	d_{max} (m)	% solid (vol)	τ_0 (Pa)	h (m)	n	$\overline{V}$ (m/s)	Fr	$\overline{V}$ (m/s) at Fr = 1.2
0.0014	0.038	20	24.6	1.35	0.0156	2.85	0.78	4.37
			21.6	1.05		2.44	0.76	3.85
	0.064	30	41.5	2.28		4.10	0.87	5.67
			36.3	1.77		3.46	0.83	5.00

sible Tapeats subcrop. Using this slope, Equation (2) yields flow depths ranging from 1.05 to 2.28 m. Using the Manning equation (3), velocities of 2.44 to 4.10 m/s were obtained. These values are within the range of answers produced by varying parameters and thus not of great significance, and the resulting Froude numbers fell significantly, ranging from 0.76 to 0.87, contrary to the desired result. These are low values for flood conditions (Barnhart, 2011b; Costa, 1987).

Another way of evaluating velocity was to substitute a Froude number of 1.2 into Equation (4). The flow depth was derived using S = 0.0014, and the equation was solved for velocity. This Fr was only slightly elevated but matched Costa's (1987) lower Froude number with the same slope. A higher value than Fr = 1.2 is hard to justify. However, the resulting velocity was 3.85 to 5.67 m/s (Table V), which are only 35% to 57% larger than the originals. Even so, these are still not as great as those seen in some of Costa's (1987) small flash flood events.

Costa (1987) correlated his lowest velocities with the lowest slopes, and the lowest Froude numbers did correspond with the lowest slopes. The lower velocities of Tables I and II suggest then that the paleoslope of the Tapeats subcrop was very low. But since plastic flows primarily acquire energy from gravity, movement over a slope of 0.0014, equivalent to 0.09%, would be very difficult to sustain over distances of 10's of meters, much less 10's of km. One way around this problem is the existence of a large, ongoing energy head behind the current, forcing the longer transport distances. Barnhart (2011b) pointed out the strong current in the London Avenue neighborhood of New Orleans was dependent not only on the hurricane but also on the size and height of Lake Pontchartrain; this large body of water was pushing through the levee breach. What was the "Lake Pontchartrain" for the Tapeats? It seems logical that it was located to the northeast, the direction of the sediment source. This is exactly the opposite direction that is offered by McKee (1945), Hereford (1977), and Rose (2006) for the transgressing ocean basin, but it needs to be considered.

Conclusion

We understand much about beaches today, from estuaries to below wave base we have seen how sediments are eroded, transported, and deposited. Bedforms and their causal conditions have been documented. A broad range of observational data is available for comparison to the basal Tapeats. If this sandstone represents a beach environment, then we must assume that the sand was deposited one wave at a time and that it was worked and reworked into its preserved bedforms. That would satisfy Hutton's first requirement.

But the paleoenvironmental option does not explain the observed sediments and bedforms of the formation. Instead, the basal Tapeats was deposited quite rapidly—between 9 and 54 m/hr, and by a plastic flow reflecting flood-flow conditions. Rose's (2006) suggestion of estuarine deposition seems plausible on the surface, but it would require a river with a depositional front of about 300 km, the distance from Grand Canyon's western mouth to the southern end of the Tapeats in central Arizona (Figure 2). This would be a river as wide as Baja, California and the Gulf of California combined! Clearly, no such river exists anywhere on Earth today, and Hutton's principle is invalidated.

Additionally, for a river to produce the necessary hyperpycnal flow, it would require a depth-averaged flow velocity of 3 m/s over a significant distance from the point of submerging up to 10's of km. Furthermore, it would have required a velocity of 15 m/s or more (Lamb et al., 2010) for the flow prior to the plunge point. Such a velocity would require a slope of 0.05 – 0.10 or higher. Yet the slope for the basal Tapeats was determined to be lower than S = 0.016 and probably in the range of 0.0025, two orders of magnitude less. Nor does that kind of flow fit with Rose's (2006, p. 234) description of "tidal channels [that] meandered and temporarily pooled and flowed."

Moreover, the erosion and deposition cycle of a beach and its associated areas suggests an ongoing process over long periods of time. But the Great Unconformity is a surface created abruptly, exhibiting only a few meters of erosional breccia in only a few isolated locations where bedforms were deposited in seconds to minutes under flood-flow conditions in a one-time event. Outside of these few isolated locations, covering a total area of less than a km^2, the overwhelming majority of the 23,000 km^2 of

the Great Unconformity shows abrupt erosion, creating a planation surface with low relief—variations of less than "a few meters per 100 m laterally" (Rose, 2006, p. 228)—and showing no erosional transition over the vast majority of that surface. Nowhere do geologists find the expected thick weathered surface. The Great Unconformity, therefore, also invalidates Hutton's dictum.

The evidence of weathering put forth by Sharp (1940) and vetted by McKee (1945) is better explained by chemical changes after burial; diagenesis in the Precambrian rocks continued as the Great Unconformity was eroded and into the deposition of the basal Tapeats (Barnhart, 2011a).

Many authors have called the breccia on the sides of monadnocks "regolith," implying a long period of weathering. But this has been shown to be a biased assumption not supported by actual field evidence. Once again, the facies model approach is shown to be camouflage for uniformitarianism.

Secular geologists have been blinded by the perceived presence of long periods of time for Earth's past. They "know" that the Tapeats must have been deposited over a long period of time and posit low energy sources as causes. However, the size and scope of the catastrophic forces required to deposit these layers can be determined by quantitative sedimentology, and these suggest a more complex origin than the facies-models approach. In the second paper of this series, it will be seen that the middle and upper Tapeats render the problem even more complicated. Regardless, it is clear that the Tapeats was deposited over a freshly eroded surface rapidly enough to "freeze" breccia cascades off of topographic highs. This was accomplished by a strong, unidirectional current with superimposed storm surge waves. Thus the Tapeats is easily interpreted within the constraints of the Genesis Flood but less easily so by uniformitarian or actualistic models.

Acknowledgments

To the two angels, Sandia and John, without whose help and encouragement this paper would never have come to be, and to the reviewer whose questions stimulated additional thought, I express my deepest thanks. You were each truly ministering spirits (Hebrews 1:14). May the Lord "establish the work of our hands for us—yes, establish the work of our hands" (Psalm 90:17, NIV).

References

Allen, J.R.L. 1976. Bedforms and unsteady processes: some concept of classification and response illustrated by common one-way types. *Earth Surface Processes* 1:361–374.

Balance, P.F. 1984. Sheet-flow-dominated gravel fans of the non-marine middle Cenozoic Simmler Formation, central California. *Sedimentary Geology* 38:337–359.

Barnhart, W.R. 2011a. How blind are we? Reading a picture. *Creation Research Society Quarterly* 47:303–305.

Barnhart, W.R. 2011b. Hurricane Katrina splay deposits: hydrodynamic constraints on hyperconcentrated sedimentation and implications for the rock record. *Creation Research Society Quarterly* 48:123–146.

Berthault, G. 2004. Sedimentological interpretation of the Tonto Group Stratigraphy (Grand Canyon Colorado River). *Lithology and Mineral Resources* 39(5):480–484.

Burgert, B.L. 1972. Petrology of the Cambrian Tapeats Sandstone, Grand Canyon, Arizona. MS thesis, Northern Arizona University, Flagstaff, AZ.

Chadwick, A.V., and M.E. Kennedy. 2001. Depositional environment of the Tapeats Sandstone in the region of Grand Canyon, Arizona. http://geology.swau.edu/faculty/tapeats.html (accessed October 2009).

Costa, J.E. 1987. Hydraulics and basin morphometry of the largest flash floods in the conterminous United States. *Journal of Hydrology* 93:313–338.

Dott, R.H., Jr. 1963. Dynamics of subaqueous gravity depositional processes. *American Association of Petroleum Geologists Bulletin* 47:104–128.

Dutton, C.D. 1882. *Tertiary history of the Grand Canyon District*. United States Geological Survey Monograph 2.

Elston, D.P., and S.L. Bressler. 1977. Paleomagnetic poles and polarity zonation from Cambrian and Devonian strata of Arizona. *Earth and Planetary Science Letters* 36:423–433.

Foley, M.G., and V.A. Vanoni. 1977. Pulsing flow in steep alluvial streams. *Journal of Hydraulics Division of American Society of Civil Engineering* 103:843–852.

Grant, G.E. 1997. Critical flow constrains flow dynamics in mobile-bed streams: a new hypothesis. *Water Resources Research* 33(2):349–358.

Hereford, R. 1977. Deposition of the Tapeats Sandstone (Cambrian) in central Arizona. *Geological Society of America Bulletin* 88:199–211.

Hutton, J. 1795. *Theory of the Earth* (cited in Holmes, A. 1965. *Principles of Physical Geology*, 2nd ed. Thomas Nelson and Sons, London, England).

Ippen, A.T. 1951. Mechanics of supercritical flow. *Transactions of the American Society of Civil Engineers* 116:268–295.

Julien, P. 1998. *Erosion and Sedimentation.* Cambridge University Press. New York, NY.

Julien, P., Y. Lan, and G. Berthault. 1994. Experiments on stratification of heterogeneous sand mixtures. *TJ* 8(1):37–50.

Karlstrom, K.E., B.R. Ilg, M.L. Williams, D.P. Hawkins, S.A. Bowring, and S.J. Seaman. 2003. Paleoproterozoic rocks of the granite Gorge. In Beuss, S.S., and M. Morales (editors), *Grand Canyon Geology*, 2nd ed., pp. 9–38. Oxford University Press, New York, NY.

Kennedy, J.F. 1963. The mechanics of dunes and antidunes in erodible-bed channels. *Journal of Fluid Mechanics* 16:521–544.

Keulegan, G.H. 1938. Laws of turbulent flow in open channels. *U.S. National*

Bureau of Standards Research Journal 21:707–741.

Kieffer, S.W. 2003. Hydraulics and geomorphology of the Colorado River in the Grand Canyon. In Beuss, S.S., and M. Morales (editors), *Grand Canyon Geology*, 2nd Edition, pp. 275–312. Oxford University Press, New York, NY.

Klein, G. deV. 1970. Depositional and dispersal dynamics of intertidal sand bars. *Journal of Sedimentary Petrology* 40(4):1095–1127.

Klevberg, P., M.J. Oard, and R. Bandy. 2009. Do paleosols indicate long ages? In Oard, M.J., and J.K. Reed (editors), *Rock Solid Answers*, pp. 93–110. Master Books, Green Forest, AR.

Lalomov, A.V. 2007. Reconstruction of paloehydrodynamic conditions during the formation of Upper Jurassic conglomerates of the Crimean Peninsula. *Lithology and Mineral Resources* 42(3):268–280.

Lamb, M.P., B. McElroy, B. Kopriva, J. Shaw, and D. Mohrig. 2010. Linking river flood dynamics to hyperpycnal-plume deposits: experiments, theory, and geological implications. *Geological Society of America Bulletin* 122:1385–1400.

Lischtvan-Lebediev. 1959. Gidrologia i gidraulika v mostovom doroshnom. *Straitielvie [m.]*. Leningrad (cited in Berthault, 2004).

Lowe, D.R. 1982. Sediment gravity flows II. Depositional models with special reference to the deposits of high-density turbidite currents. *Journal of Sedimentary Petrology* 52:279–297 (cited in Shanmugam, 1996).

Marusic, I., R. Mathis, and N. Hutchins. 2010. Predictive model for wall-bounded turbulent flow. *Science* 329:193–196.

McBride, E.F., R.G. Shepherd, and R.A. Crowley. 1975. Origin of parallel near-horizontal laminae by migrating of bedforms in a small flume. *Journal of Sedimentary Petrology* 45:132–139.

McKee, E.D. 1945. Part I: Stratigraphy and ecology of the Grand Canyon Cambrian. In *Cambrian History of the Grand Canyon Region*. Carnegie Institute of Washington Publication 563.

McKee, E.D., E.J. Crosby, and H.L. Berryhill, Jr. 1967. Flood deposits, Bijou Creek, Colorado, 1965. *Journal of Sedimentary Petrology* 37:829–851.

McLane, M. 1995. *Sedimentology*. Oxford University Press, New York, NY.

Middleton, L.T., and D.K. Elliot. 2003. Tonto Group. In Beuss, S.S., and M. Morales (editors), *Grand Canyon Geology*, 2nd ed., pp. 90–106. Oxford University Press, New York, NY.

Nichols, G. 1999. *Sedimentology and Stratigraphy*. Blackwell Publishing, Boston, MA.

Noble, L.F. 1914. The Shinumo Quadrangle, Grand Canyon District, Arizona. *USGS Bulletin* 549.

Noble, L.F. 1922. A section of the Paleozoic formation of the Grand Canyon at the Bass Trail. *USGS Professional Paper* 131-B:2393 (cited in McKee, 1945).

Oard, M.J. 2010. Is the K/T the post-Flood boundary? Part I: Introduction and the scale of sedimentary rocks. *Journal of Creation* 24(2):98.

Pierson, T.C. and J.E. Costa. 1987. A rheologic classification of subaerial sediment water flows. In Costa, J.E. and G.F. Wiecyorek (editors). *Debris Flows/Avalanches: Process, Recognition, and Mitigation*, pp. 1–12. Geological Society of America, Boulder, CO.

Postma, G., W. Nemec, and K.L Kleinspehn. 1988. Large floating clasts in turbidites: a mechanism for their emplacement. *Sedimentary Geology* 58:47–61.

Rose, E.C. 2006. Nonmarine aspects of the Cambrian Tonto Group of the Grand Canyon, USA, and broader implications. *Paleoworld* 15:223–241.

Rubin, D.M., and D.S. McCulloch. 1980. Single and superimposed bedforms: a synthesis of San Francisco Bay and flume observations. *Sedimentary Geology* 26:207–231.

Schumm, S.A., and H.R. Khan. 1972. Experimental study of channel pattern. *GSA Bulletin* 83:1755–1770.

Scott, K.M., J.W. Vallance, and P.T. Pringle. 1995. *Sedimentology, Behavior, and Hazards of Debris Flows at Mount Rainer, Washington*. United States Geological Survey Professional Paper 1547. Washington, DC.

Shanmugam, G. 1996. High-density turbidity currents: are they sandy debris flows? *Journal of Sedimentary Research* 66(1):2–10.

Sharp, R.P. 1940. Ep-Archean and Ep-Algonkian erosion surfaces, Grand Canyon, Arizona. *GSA Bulletin* 51:1235–1270.

Smith, G.A. 1986. Coarse-grained nonmarine volcaniclastic sediments: terminology and depositional process. *GSA Bulletin* 97:1–10.

Smith, G.A. 1987. Sedimentology of volcanism-induced aggradation in fluvial basins: examples from the Pacific Northwest, U.S.A. In Ethridge, F.G., R.M. Flores, and M.D. Harvey (editors), *Recent Developments in Fluvial Sedimentology: Contributions from the Third International Fluvial Sedimentology Conference*, pp. 217–228. Society of Economic Paleontologists and Mineralogists Special Publication 39, Tulsa, OK.

Smith, N.D. 1971. Pseudo-planar cross-stratification produced by very low amplitude sand waves. *Journal of Sedimentary Petrology* 41:69–73.

Sohn, Y.K. 2000. Depositional processes of submarine debris flows in the Miocene fan deltas, Pohang Basin, SE Korea, with special reference to flow transformation. *Journal of Sedimentary Resources* 70:491–503.

Sohn, Y.K., M.Y. Choe, and H.R. Jo. 2002. Transition from debris flow to hyperconcentrated flow in a submarine channel (the Cretaceous Cerro Toro Formation, southern Chile). *Terra Nova* 14:405–415.

Walcott, C.D. 1890. The fauna of the Lower Cambrian, or Ollenellus zone. *USGS 10th Annual Report*:509–760.

Wanless, H.R. 1973. Cambrian of the Grand Canyon. A reevaluation of the depositional environment. Ph.D. Diss., John Hopkins University, Baltimore, MD. (cited in Hereford, 1977, and Middleton and Elliot, 2003).